

UNCLASSIFIED

AD NUMBER

AD843056

LIMITATION CHANGES

TO:

Approved for public release; distribution is unlimited.

FROM:

Distribution authorized to U.S. Gov't. agencies and their contractors; Critical Technology; NOV 1968. Other requests shall be referred to Air Force Rocket Propulsion, Lab., Research and Technology Div., Attn: RPPR-STINFO, Edwards AFB, CA 93523. This document contains export-controlled technical data.

AUTHORITY

AFRPL ltr dtd 28 Mar 1974

THIS PAGE IS UNCLASSIFIED

AFRPL-TR-68-205

AGC 1082-81F

AD843056

MICROSCOPIC AND MICROCHEMICAL STUDY  
OF AGED SOLID PROPELLANT GRAINS

H. Moe, A. J. Di Milo and J. L. McGurk  
Chemical and Physical Sciences Section  
Aerojet-General Corporation  
Sacramento, California

Final Technical Report AFRPL-TR-68-205

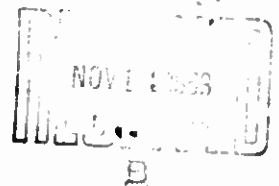
November 1968

This document is subject to special export controls and each transmittal to foreign governments or foreign nationals may be made only with prior approval of AFRPL (RPFEL-STINFO), Edwards, California 93523.

Sponsored By

Air Force Rocket Propulsion Laboratory  
Research and Technology Division  
Edwards, California

Air Force Systems Command, United States Air Force



RESTI		WHITE SECTION 11
DDC		BLUE SECTION 11
UNANNOUNCED		
JUSTIFICATION		
BY . . . . .		
DISTRIBUTION/AVAILABILITY CODE		
DIST.	AVAIL.	REMARKS
2		

"When U. S. Government drawings, specifications, or other data are used for any purpose other than a definitely related Government procurement operation, the Government thereby incurs no responsibility nor any obligation whatsoever, and the fact that the Government may have formulated, furnished, or in any way supplied the said drawings, specifications, or other data, is not to be regarded by implication or otherwise, or in any manner licensing the holder or any other person or corporation, or conveying any rights or permission to manufacture, use, or sell any patented invention that may in any way be related thereto."

AFRPL-TR-68-205

**MICROSCOPIC AND MICROCHEMICAL STUDY  
OF AGED SOLID PROPELLANT GRAINS**

**H. Moe, A. J. Di Milo and J. L. McGurk**

This document is subject to special export controls and each transmittal to foreign governments or foreign nationals may be made only with prior approval of AFRPL (RPPR-STINFO), Edwards, California 93523.

FOREWORD

This technical report was prepared under Contract No. AF 04(611)-11637 as fulfillment of the requirements of Project No. 3148 of the Air Force Rocket Propulsion Laboratory, Research and Technology Division, Air Force Systems Command, Edwards, California. The work was performed in the Chemical and Physical Sciences Section of the Research and Technology Department, Aerojet-General Corporation, Sacramento, California. This report was designated Aerojet-General Report 1082-81F and covers the progress made in the period 18 July 1966 to 17 July 1968. This project was monitored by Robert Bargmeyer, Capt., and David J. Yardley, 2/Lt., USAF/RPCS.

Acknowledgement is made to the following persons who have contributed materially to the work performed:

At Aerojet-General

J. T. Becerril, Senior Laboratory Technician, B. B. White, Manager, Mechanical Properties Laboratory, H. D. Orcutt, Electron Microscopist, W. Hartmann, Hawk Projects.

At Hill Air Force Base

Mr. Leo Granath

At Thiokol Chemical Corporation

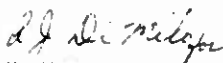
Mr. Paden

Special acknowledgement is made to Mr. J. L. McGurk who was principal investigator for the inception of this program until November 1967.

Prepared by:

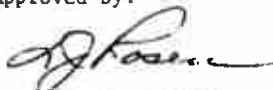


A. J. Di Milo  
Program Manager



H. Moe  
Principal Investigator

Approved by:



L. J. Rosen, Manager  
Solid Propellant Research Group  
Research & Technology Department

This technical report has been reviewed and is approved.

W. H. Ebelke, Colonel, USAF  
Chief, Propellant Division

#### ABSTRACT

Microscopic examination of thin sections of aged polyurethane propellant from a field aged Polaria motor revealed the presence of high refractive index reaction sites surrounding aluminum particles. Chemical analyses of these sites revealed them to be composed of polyurethane binder. Color sites in a Hawk field aged motor were found by microscopic examination and chemical analysis of these sites showed them to be due to the presence of iron in different oxidation states. The source of the iron is the iron acetylacetonate used as a curing catalyst.

Model propellant grains were made to simulate conditions for the generation of reaction sites and the formation and growth of the sites were followed by mapping. Correlation of reaction site formation with mechanical properties of the propellant was unsuccessful because the propellants available for study (up to 7 years old) showed no real loss of mechanical and ballistic capability. The reaction sites portend changes which will occur over a period of time not now available for study.

The chemical mechanism of the aging was defined and expressed by chemical equations.

## TABLE OF CONTENTS

	<u>Page</u>
I. MICROSCOPIC STUDIES	1
A. Introduction	1
B. Reaction Sites	1
1. Refractive Type of Reaction Sites	1
a. General	3
b. Planimetric Analysis of Three Month Aging Samples	6
c. Variation of Reaction Site Relative Concentration with Storage Temperatures	6
d. Discussion of Map Data	17
e. Planimetric Analysis of Refractive Sites in Model Igniter Grains Aged Six Months	21
f. Refractive Site Absolute Volume	28
g. Size Distribution	29
2. Color Type Reaction Sites	32
a. Description of Sites in Field Aged Motor	32
b. Colored Reaction Sites in Model Bipropellant Grains	35
3. Conclusions from Microscopic Studies	45
II. CHEMICAL STUDIES	46
A. Introduction	46
B. Chemical Analysis of Polaris Cycling Unit	46
1. Analysis of the EDC Soluble Fraction	46
2. Analysis of the Polaris Refractive Sites	48

## TABLE OF CONTENTS (Cont)

	<u>Page</u>
C. Chemical Analysis of Hawk Propellant	52
1. Sample Preparation	52
2. Methylene Chloride Extracts	53
a. Analysis for Plasticizer	53
b. Analysis of FeAA	53
3. Aqueous Extracts	55
D. Mechanisms of Iron Migration and Chemical Changes	55
1. Stability of a Model Urethane and a Model Urea	58
E. Chemical Analysis of a PBAN-Epoxy Propellant	58
III. MECHANICAL AND BALLISTIC PROPERTIES AND REACTION SITES OF PROPELLANTS	61
A. The Hawk Propellant System	61
B. The Polaris and Minuteman Igniter Propellant Systems	61
IV. SUMMARY	66
A. The Mechanism of Site Formation	66
B. Recommendations	67
C. Experimental Techniques	67



## LIST OF TABLES

<u>Table</u>		<u>Page</u>
I	Storage Conditions and Aging Time for Model Grains	3
II	Relative Volume Percent of Refractive Sites in Model Igniter Aged for 3 and 6 Months	28
III	Relative and Absolute Volume Concentration of Refractive Sites	28
IV	Chemical Analyses of Hawk Surveillance Motor	54
V	Mechanical Properties of Full Scale Hawk Field Motors	62
VI	Mechanical Properties of Full Scale Hawk Field Motors	63
VII	Mechanical Properties of Full Scale Hawk Field Motors	64
VIII	Mechanical Properties of Polaris Propellant ANP-2639 Aged 65 Months in Field	64
IX	Mechanical Properties of Model Minuteman Igniter Propellant ANP-2758 Mod 11	65

## LIST OF FIGURES

<u>Figure</u>		<u>Page</u>
1	A Refractive Site in Transmitted Light	2
2	Reaction of Aluminum	4
3	Polished and Etched Aluminum Particle Showing Grain Boundaries	5
4	Location of Reactive Sites in Sample From Model Igniter Grain Aged 3 Months at 120°F	7
5	Number of Reaction Sites Per Unit Circle in Model Igniter Aged 3 Months, 120°F	8
6	Number Frequency Map, Model Igniter Grain Aged 3 Months, 120°F	9
7	Volume Concentration Map, Model Igniter Grain Aged 3 Months, 120°F	10
8	Volume Concentration Contour Map Model Igniter Grain, Aged 3 Months, 120°F	11
9	Volume Concentration Map, Model Igniter Grain Aged 3 Months, 120°F	12
10	Volume Concentration Contour Map, Model Igniter Grain Aged 3 Months, 120°F	13
11	Volume Concentration Contour Map, Model Igniter Grain Aged 3 Months, 110°F	14
12	Volume Concentration Contour Map, Model Igniter Grain Aged 3 Months, 110°F	15
13	Volume Concentration Contour Map, Model Igniter Grain, Aged 3 months, 130°F	16
14	Relative Volume Concentration of Reaction Sites for A Model Igniter Grain Aged for 3 Months	18
15	Distribution of Refractive Reaction Sites in Sealed Igniter Motor, 3 Months at 125°F	19

# LIST OF FIGURES (Cont)

<u>Figure</u>		<u>Page</u>
16	Distribution of Refractive Reaction Sites in Field Igniter Motor, 1 Year Old	20
17	Isopleth Map, Model Igniter Grain 6 Months 110°F, A	22
18	Isopleth Map Model Igniter Grain 6 Months 110°F, B	23
19	Isopleth Map, Model Igniter Grain 3/3 Months 120/50°F, B	24
20	Isopleth Map, Model Igniter Grain 6 Months 130°F, 2	25
21	Relative Volume Concentration of Refractive Sites in Model Igniter Grains Aged 3 and 6 Months	26
22	Percent Increase in Reaction Site Volume Between 3 and 6 Months Samples	27
23	Histogram of Refractive Site Size in Model Igniter Grains Aged 6 Months	30
24	Probability Plot of Refractive Site Size in Model Igniter Grain Aged 6 Months	31
25	Light Scattering Around Colored Reaction Sites	33
26	Hawk Field Motor, 5-1/2 Yrs, Distribution of Colored Reaction Sites at Forward End	34
27	Reaction Sites, Refractive and Colored Typea (320 X)	36
28	Schematic Isopleth Map Showing Location of Colored and Refractive Reaction Sites in a Bipropellant Grain Section	37
29	Grain Section of Model Bipropellant Grain Showing Location of Mapped Area	39
30	Frequency Map of All Colored Reaction Sites in Model Bipropellant Grain Aged 9 Months at 120°F	40
31	Frequency Map of Clear, Yellow-Green Reaction Sites at 120°F in Model Bipropellants Aged 9 Months	41
32	Frequency Map of Reaction Sites with Green Refractive Gel in Model Bipropellant Grain Aged 9 Months at 120°F	42

# LIST OF FIGURES (Cont)

<u>Figure</u>		<u>Page</u>
33	Frequency Map of Reaction Sites with a Green and Red-Orange Stain in Model Bipropellant Aged 9 Months at 120°F	43
34	Frequency Map of Reaction Sites with a Red Orange Gel and a Green-Brown Stain in Model Bipropellant Aged 9 Months at 120°F	44
35	Thin-Layer Silica-Gel Chromatographs of Degraded Propellant (See Text) Fractions	47
36	Typical Infrared Spectrum of Material from Degraded Polaris Binder Chromatographed on $Al_2O_3$ Column	49
37	Infrared Spectrum of Reaction Product of Polypropylene Glycol and Toluene Diisocyanate	50
38	Photomicrographs of the Separation of $NH_4ClO_4$ and Aluminum from Reaction Site from Polaris Cycling Unit	51

MICROSCOPIC AND MICROCHEMICAL STUDY  
OF AGED SOLID PROPELLANT GRAINSI. MICROSCOPIC STUDIES

## A. INTRODUCTION

Microscopic reaction sites are localized spots in aged propellants with abnormal optical properties when compared to the optical constants of unaged propellants. Prior studies under several aging surveillance programs had revealed that the reaction sites were observed in propellants made of polyurethane binder,  $\text{NH}_4\text{ClO}_4$ , Al, and FeAA. These reaction sites were detected after an induction period, increased with aging period, and attained maximum development after five to seven years. The objective of this program was to duplicate these results in model motors with selected components and to identify the specific compounds required to reproduce the optical phenomena. Extensive studies were made of the optical characteristics of these reaction sites and these studies led to conclusions about the relationships between reaction sites and aging. These conclusions were further explored by conducting chemical analyses in attempts to more accurately define the aging mechanism of propellants.

## B. REACTION SITES

There are two basic types of reaction sites, one characterized by a noticeable change in the refractive index of the binder, and the other characterized by a series of color absorption shells in the binder. Both reaction sites occur as shells centered about aluminum particles and attain a size that averages about 150 microns. These two types of reaction sites also have characteristically different distributions within the grain. The sites with altered refractive index attain their maximum development near the bore surface of the grain. The sites with color absorption shells occur in bipropellants and attain their most characteristic color pattern near the bipropellant interface. The refractive type reaction sites were studied using a Polaris motor with propellant ANP-2639 which had been field aged for 7-1/2 years and a second stage Minuteman Wing II igniter motor with propellant ANP-2758 Mod II aged for one year. Studies of colored type reaction sites were made using a Hawk motor with propellant ANP-2832 Mod I (sustainer) and ANP-2830 Mod I (booster) which had been field aged for 5-1/2 years.

1. Refractive Type of Reaction Sites

A generalized structure for the refractive type reaction site consisted of a central aluminum particle surrounded by a clear, gummy shell which in turn was surrounded by an opaque shell. A thin section of the Minuteman igniter grain was examined at the same magnification under four types of transmitted light (Figure 1); (a) intense convergent light which showed the lack of opaque material, (b) plane polarized light which showed

# A REFRACTIVE SITE IN TRANSMITTED LIGHT



a. Convergent



b. Plane polarized

125X



c. Dark field



d. Doubly polarized

the multiple phase composition of transparent material, (c) dark field phase which showed the altered refractive index of the transparent material, and (d) doubly polarized light which showed the presence of several birefringent crystals of fine ammonium perchlorate. Numerous variations of these refractive sites occur; some are optically very clear and others are complex, but most have a well defined boundary which permitted measurement of their area with a grid eyepiece.

In some reaction sites, the aluminum had been corroded away until only a very fine network of aluminum mesh was seen, Figure 2-a. At other reaction sites, the aluminum surface was highly serrated, indicating surface corrosion, Figure 2-b. To investigate possible reasons for the variable corrosion process, aluminum particles were embedded in an epoxy, polished and etched, Figure 3. In general, some of these embedded aluminum particles were composed of a few grains while others were multigranular; surface corrosion occurred where the particle had a few grains and the network corrosive process occurred on those with the multiple grain structure. The fine aluminum particles were observed to be mostly single grains. Some of the ammonium perchlorate crystals apparently dissolve and some of the one to five micron size  $\text{NH}_4\text{ClO}_4$  particles are redistributed.

#### a. General

The objective of this phase of the program was the application of microscopic methods for determination of reaction site concentration, distribution, and nucleation rate as a function of propellant storage temperature, time, and environment.

Samples used in this study were from model propellant grains whose formulation was identical to the Minuteman igniter propellant, ANP-2758 Mod II. Two motors of 3KS-1000 size were prepared in split Micarta cylinders, 4.75 inches in diameter and 18.6 inches long, with a gear core. These were cut in half providing four grains which were placed in ovens of different temperatures (Table I).

TABLE I

STORAGE CONDITIONS AND AGING TIME FOR MODEL GRAINS<sup>a</sup>

Grain No.	Temp., °F	Age at Sample Time, days	
		3 month	6 month
1	180	89	169
2	120 <sup>b</sup>	84	169
3	110	89	169
4	130	84	169

<sup>a</sup>Second stage Minuteman Wing II igniter propellant, ANP 2758 Mod II

<sup>b</sup>Stored at 120°F for 108 days, then kept at 50°F

# REACTION OF ALUMINUM



a

125X

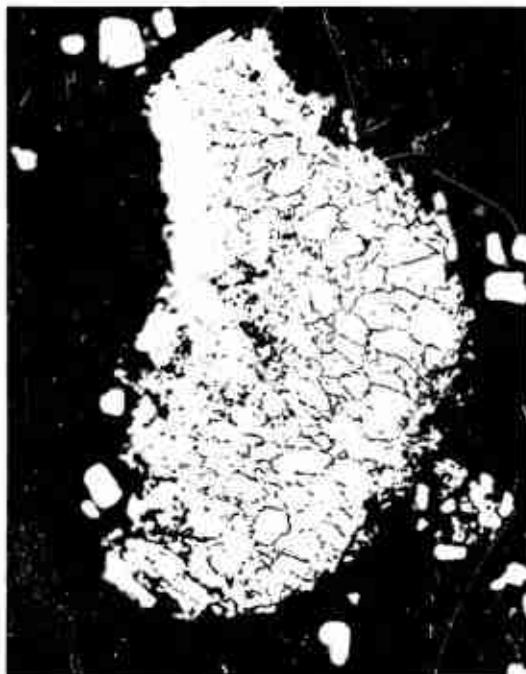


b

500X



POLISHED AND ETCHED ALUMINUM PARTICLE  
SHOWING GRAIN BOUNDARIES



500X

#### b. Planimetric Analysis of Three Month Aging Samples

Samples were taken with a cork borer along a radial axis one inch from the end of the model igniter grain. These were microtomed and mounted on microscope slides so that there was a continuous series of thin sections from case wall to ray tip.

The thin sections were mounted on the mechanical stage of the microscope, the entire section was traversed and the coordinates of each refractive site recorded. A calibrated grid eyepiece was used to determine the size range of the site which was recorded along with the coordinates.

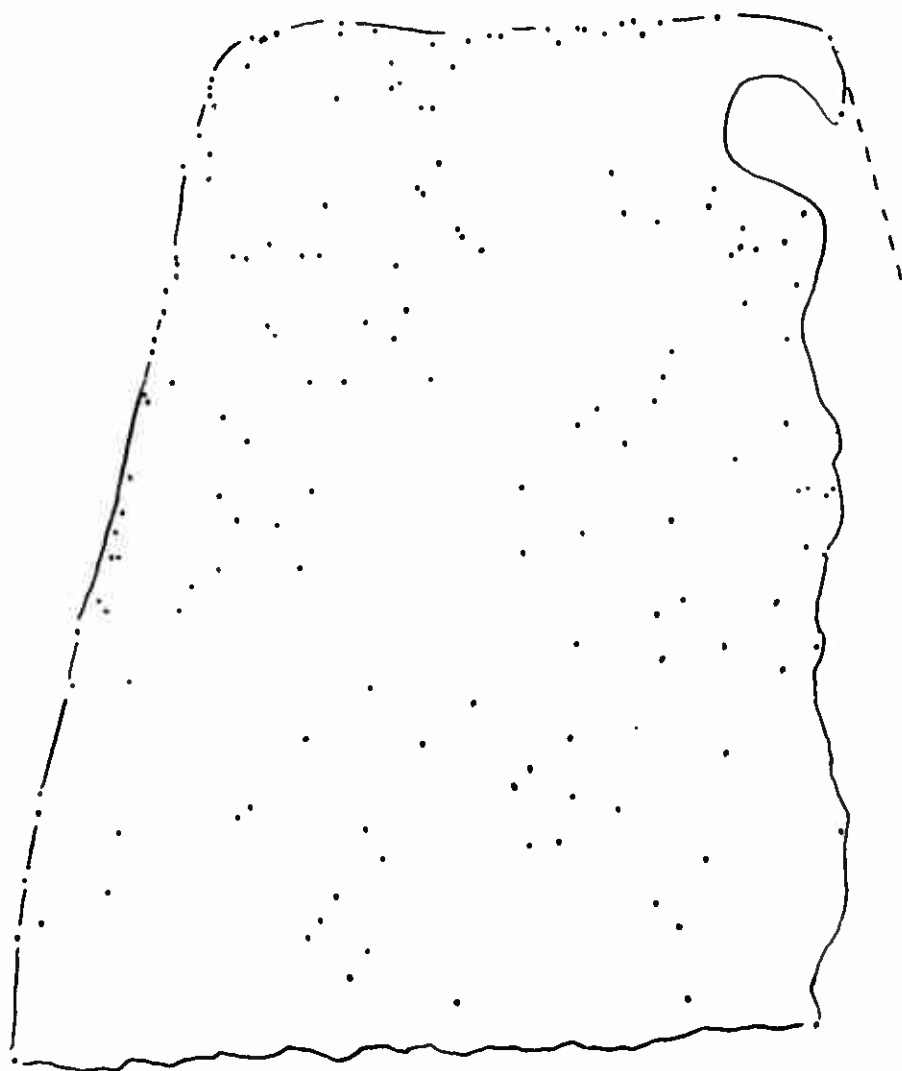
The coordinate data were plotted on a centimeter grid at a scale giving approximately a 1:10 enlargement, and a color code was used to designate size ranges. The procedure is demonstrated with the 120°F sample in Figure 4 where the points are plotted without size designation. A transparent countout overlay and a 5/8" diameter template circle were placed over Figure 4 and the points within the circle were totaled. This was repeated by moving the circle one centimeter at a time, until the whole figure was covered. The number of reaction sites for each position of the template circle was then recorded on a number overlay (Figure 5). Another transparent overlay was placed on the number map and the points of equal concentration contoured in. The resulting map, Figure 6, shows the frequency concentrations of reaction sites over the sample in question.

The site size was taken into account by assigning a number weight to each reaction site according to its area. The total weighted values of all the points within the counting circle were recorded on a volume concentration map, Figure 7, and then contoured on a map overlay, Figure 8. The weighted map overlay thus shows values related to the concentration by volume of reaction sites per unit circle in a section of standard thickness. When Figure 8 is compared to Figure 4, the contours do not adequately portray the high frequency of points along the left side. Because there is no direct correlation between the frequency of occurrence and the size of reaction sites, a random size distribution of the sites leads to the conclusion that areas of higher frequency yield proportionately higher volume concentration of sites. Therefore, the plot grid was reduced to 0.25 cm squares and the counting circle size to 1.0 cm and the procedure repeated to produce the countout of Figure 9 and map in Figure 10. Figure 10 gives a more realistic representation of both the frequency and volume concentration.

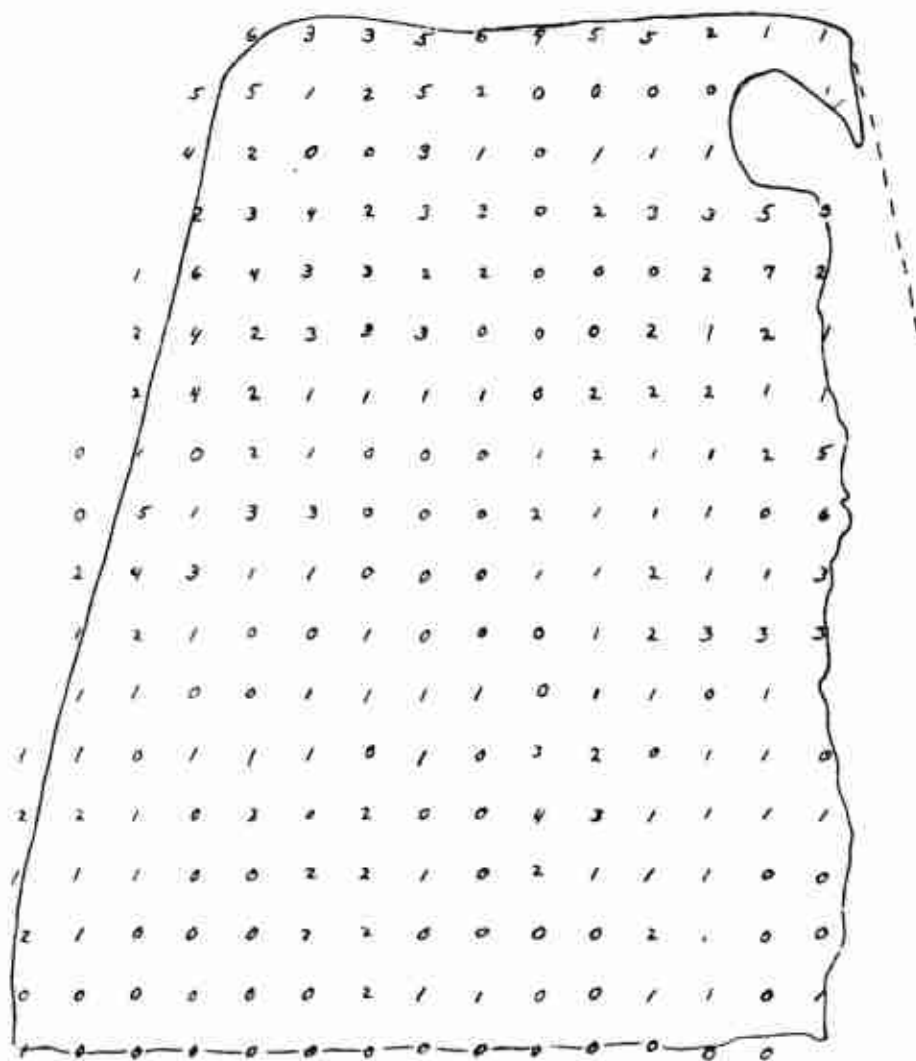
#### c. Variation of Reaction Site Relative Concentration with Storage Temperatures

The mapped data of reaction site relative volume concentration from Igniter Grains 2, 3, and 4 are shown in Figures 10, 11, 12, and 13. Figures 11 and 12 represent a continuous strip of propellant from case wall to ray tip for grain aged for 3 months at 110°F. The contour interval

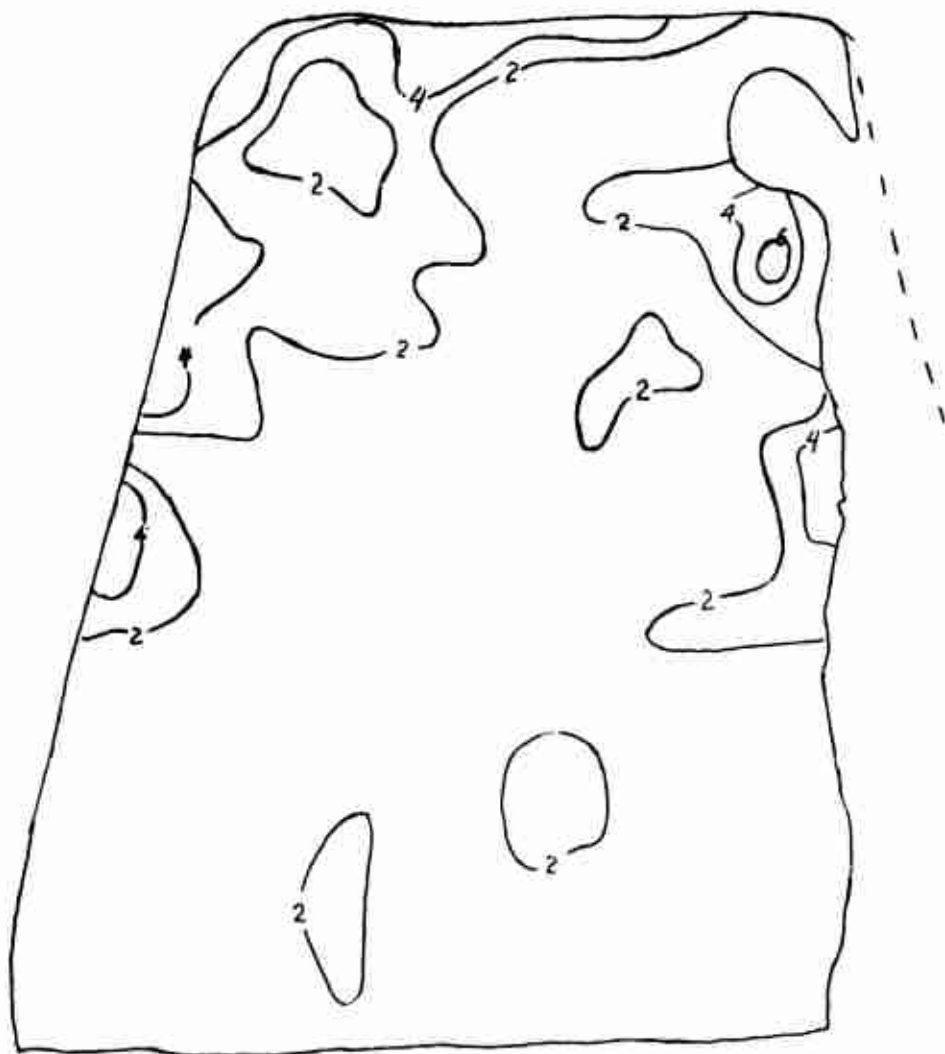
LOCATION OF REACTIVE SITES IN SAMPLE FROM MODEL IGNITER  
GRAIN AGED 3 MONTHS AT 120°F



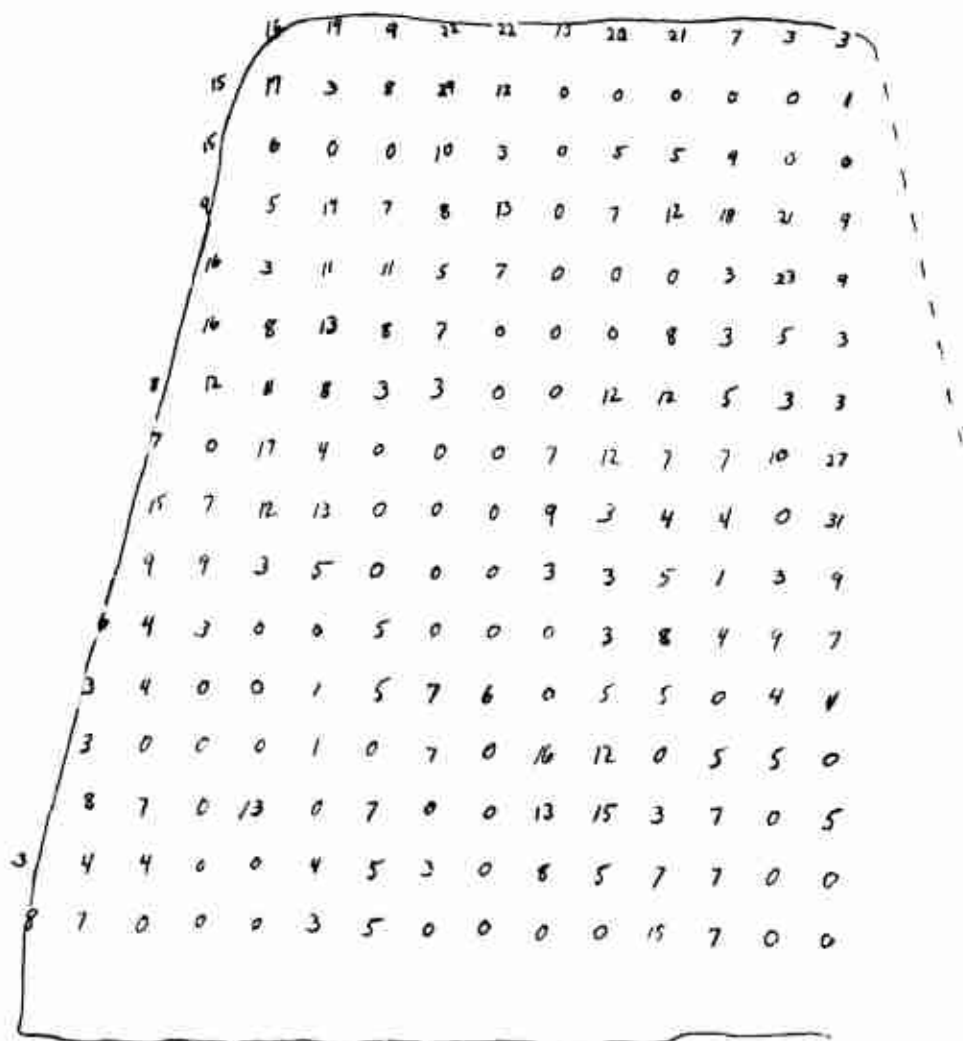
NUMBER OF REACTION SITES PER UNIT CIRCLE  
IN MODEL IGNITER  
AGED 3 MONTHS, 120°F



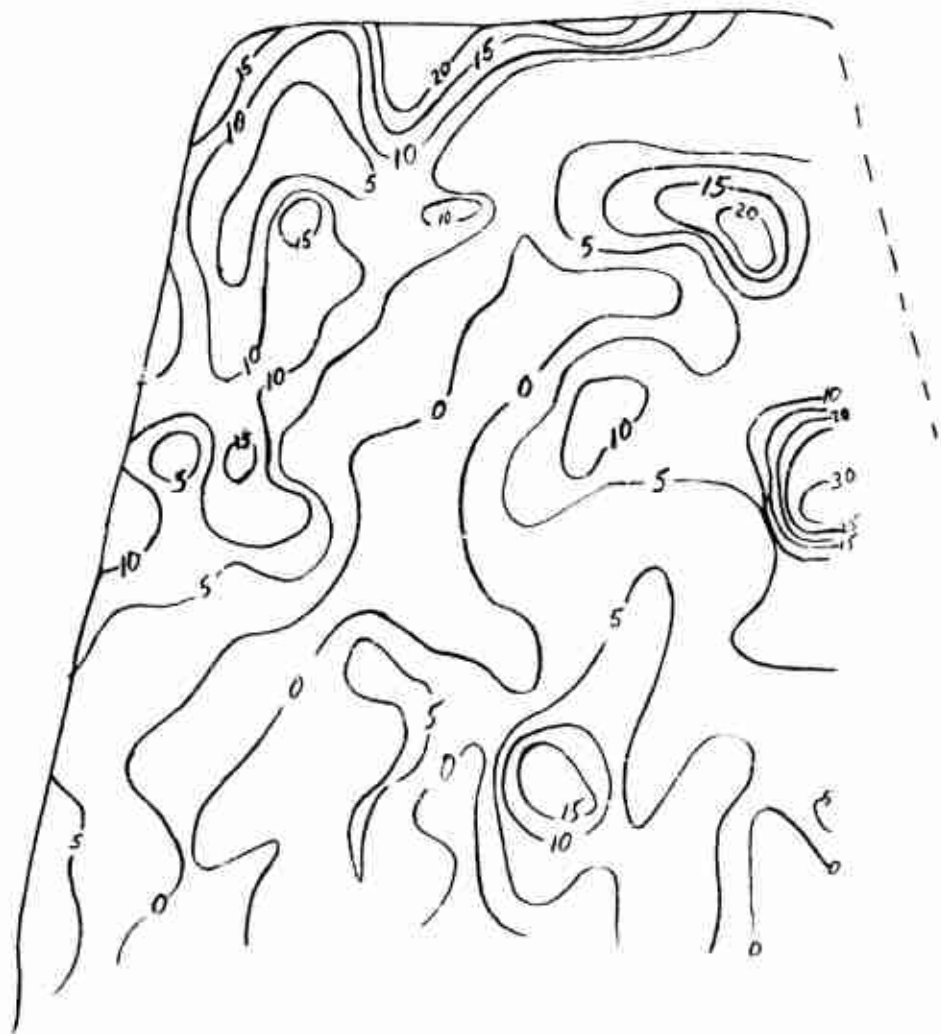
NUMBER FREQUENCY MAP, MODEL IGNITER GRAIN  
AGED 3 MONTHS, 120°F



VOLUME CONCENTRATION MAP, MODEL IGNITER GRAIN  
AGED 3 MONTHS, 120°F



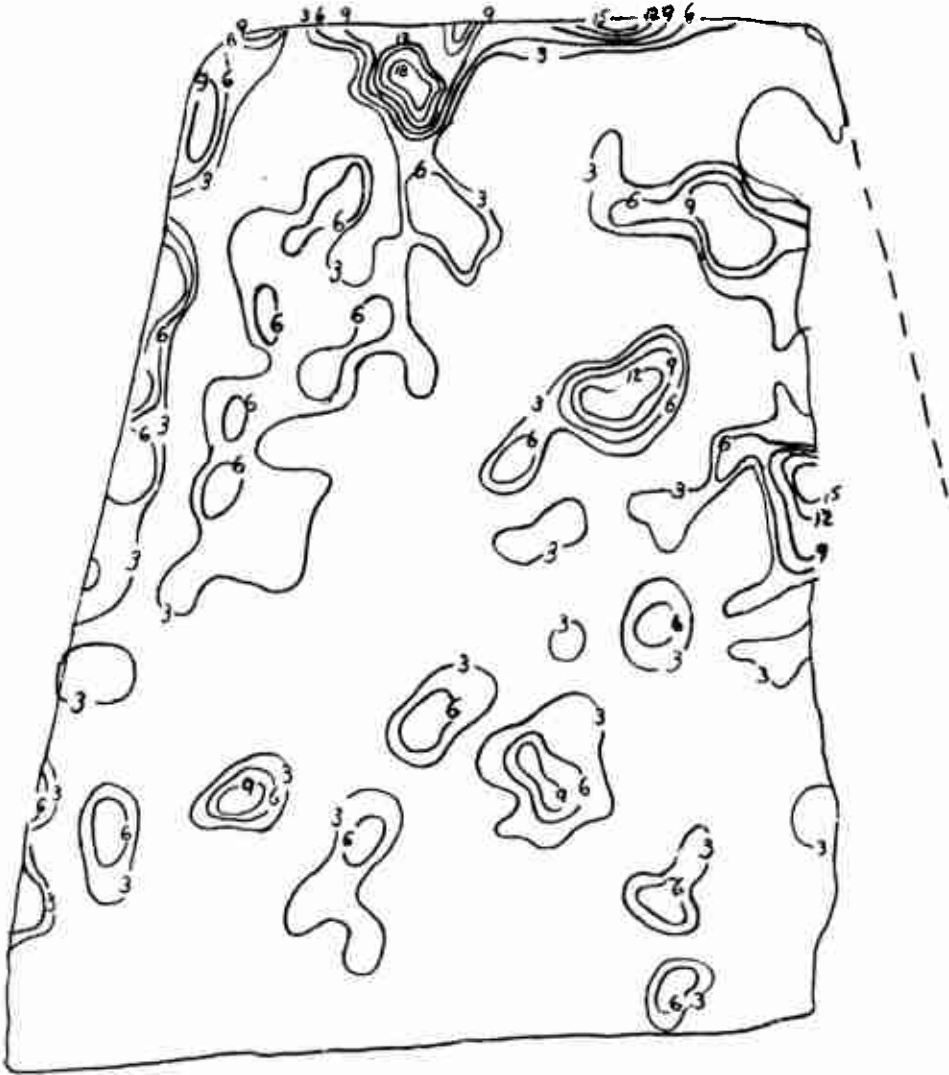
VOLUME CONCENTRATION CONTOUR MAP MODEL IGNITER GRAIN,  
AGED 3 MONTHS, 120°F



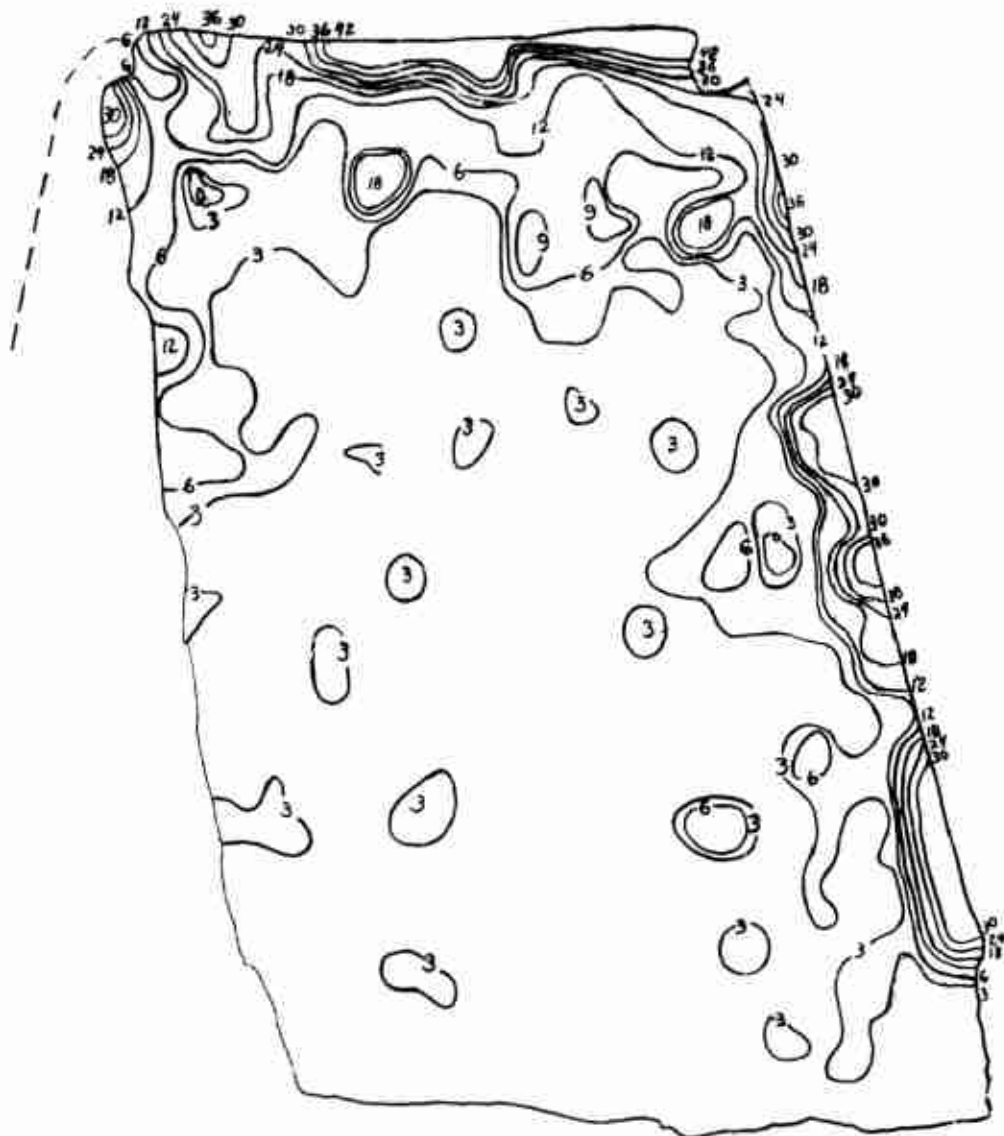
[illegible]



VOLUME CONCENTRATION CONTOUR MAP, MODEL IGNITER GRAIN  
AGED 3 MONTHS, 120°F



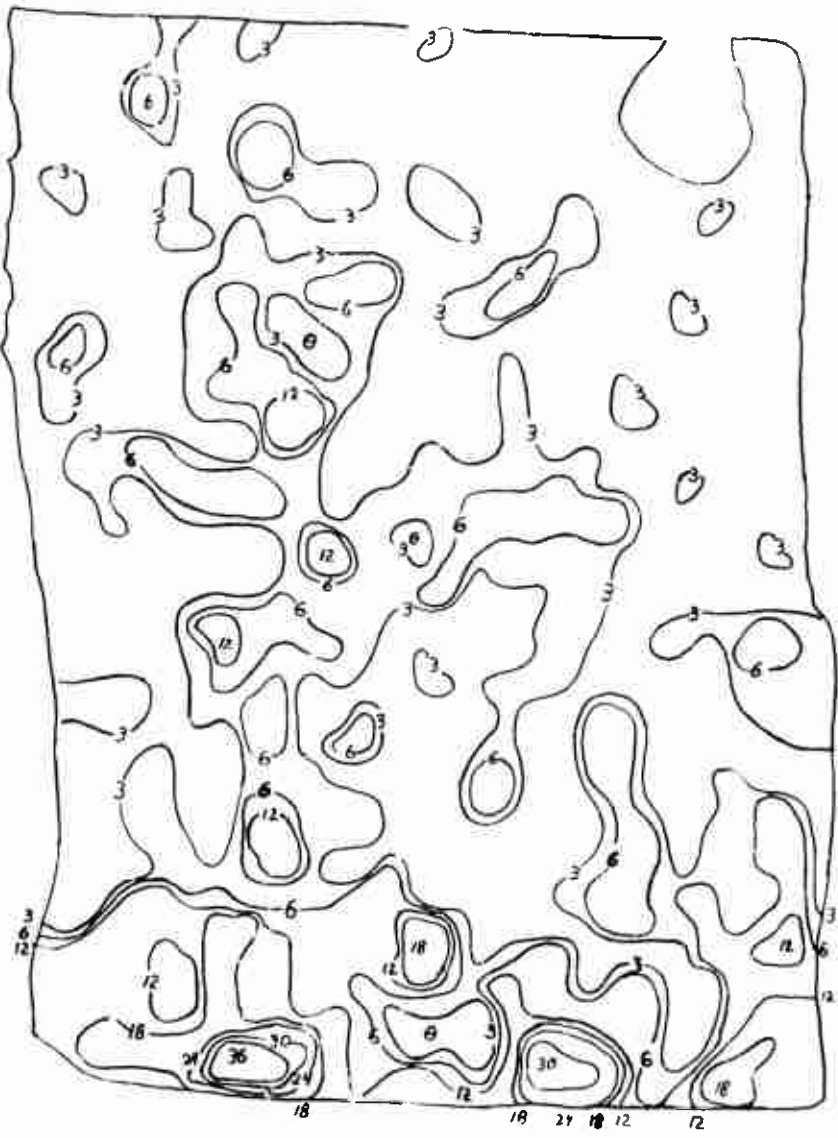
VOLUME CONCENTRATION CONTOUR MAP, MODEL IGNITER GRAIN  
AGED 3 MONTHS, 110°F



Continued on Figure 12

VOLUME CONCENTRATION CONTOUR MAP, MODEL IGNITER GRAIN  
AGED 3 MONTHS, 110°F

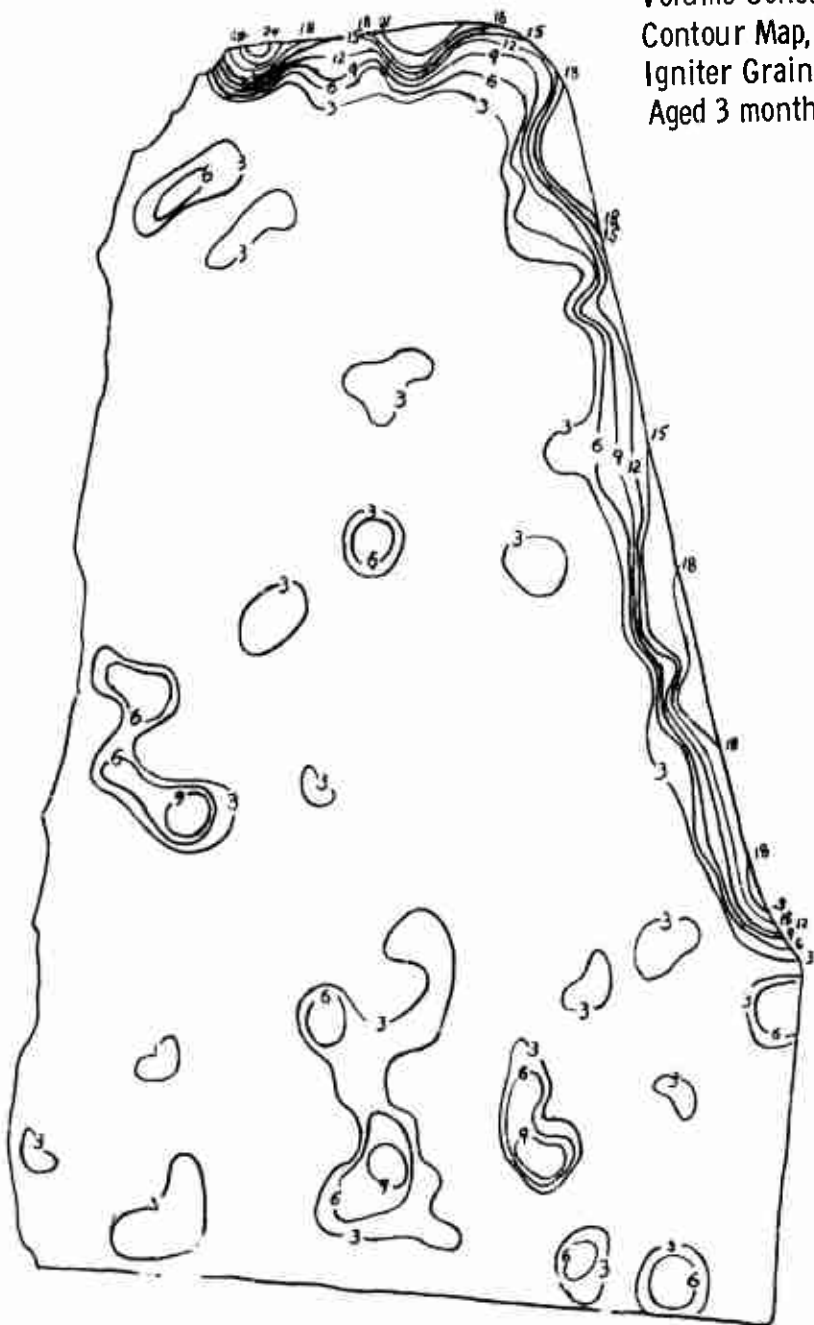
Continuation of Figure 11



Case Wall

FIGURE 12

Volume Concentration  
Contour Map, Model  
Igniter Grain,  
Aged 3 months, 130°F



on Figures 10 and 13 for propellant aged 3 months at 120° and 130°F, respectively, is 3%, while on Figures 11 and 12 the contour interval is 6%. In all figures the zero line is omitted and a 3% contour is the base line. Although a uniform contour interval is useful for comparison purposes, the contours are used here to serve as area boundaries and are those expedient for examination of variables. For example, use of the 3% contour interval on Figure 11 would require doubling the scale, the labor, and time of analysis.

While the contour maps (Figures 10 through 13) are useful to show the distribution of sites within a given sample, they are not most suitable for comparison of one sample with another. For comparison of one sample with another it was more convenient to compare the fractions of the area covered by contours relative to the total area of the map. Because this fraction is proportional to the actual volume concentration of the sites (see Table III), the fraction was termed the relative volume concentration. In actuality, the fraction is simply a ratio of areas derived (as indicated below) from the contour maps.

For each of the contour maps, the area within each contour interval was determined with a planimeter, summed, and the total divided by the sample area. These relative values, however, must not be confused with the actual volumes which are much less (less than 1%). The actual volume concentrations of the sites were derived as indicated in Section I.B.1.f.

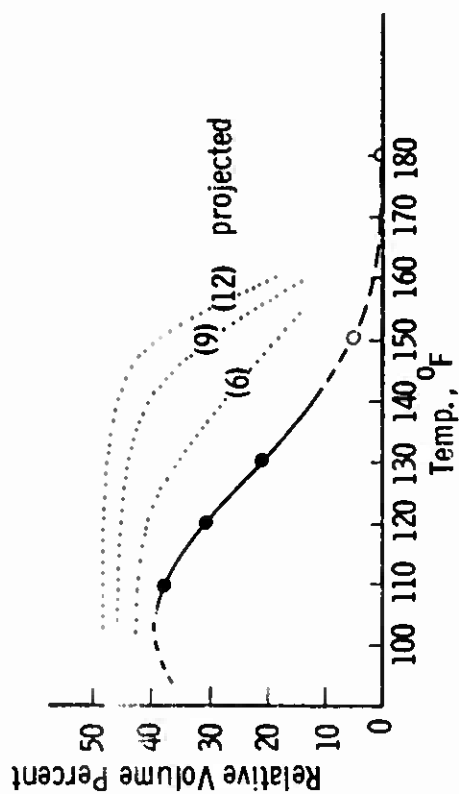
The planimetric analysis yielded relative values of 37.9% at 110°F, 31.3% at 120°F, and 21.2% at 130°F. These are plotted on a graph in Figure 14 showing reaction site concentration (in relative values) versus temperature for the first 3-month period. The point at 180°F is from the first model igniter grain where no reaction sites were visible in the ray section. The point at 150°F is an estimate from some previous work on a Polaris formulation with a composition essentially similar to that for the model igniter grains.

Figure 15 shows the location and size of refractive sites for a Minuteman Igniter Motor aged in a sealed atmosphere at 125°F for 3 months, and Figure 16 is a similar plot for a Minuteman Igniter Motor that had been in a silo for about one year. The scale in Figures 15 and 16 is the same as that in Figures 10 through 13.

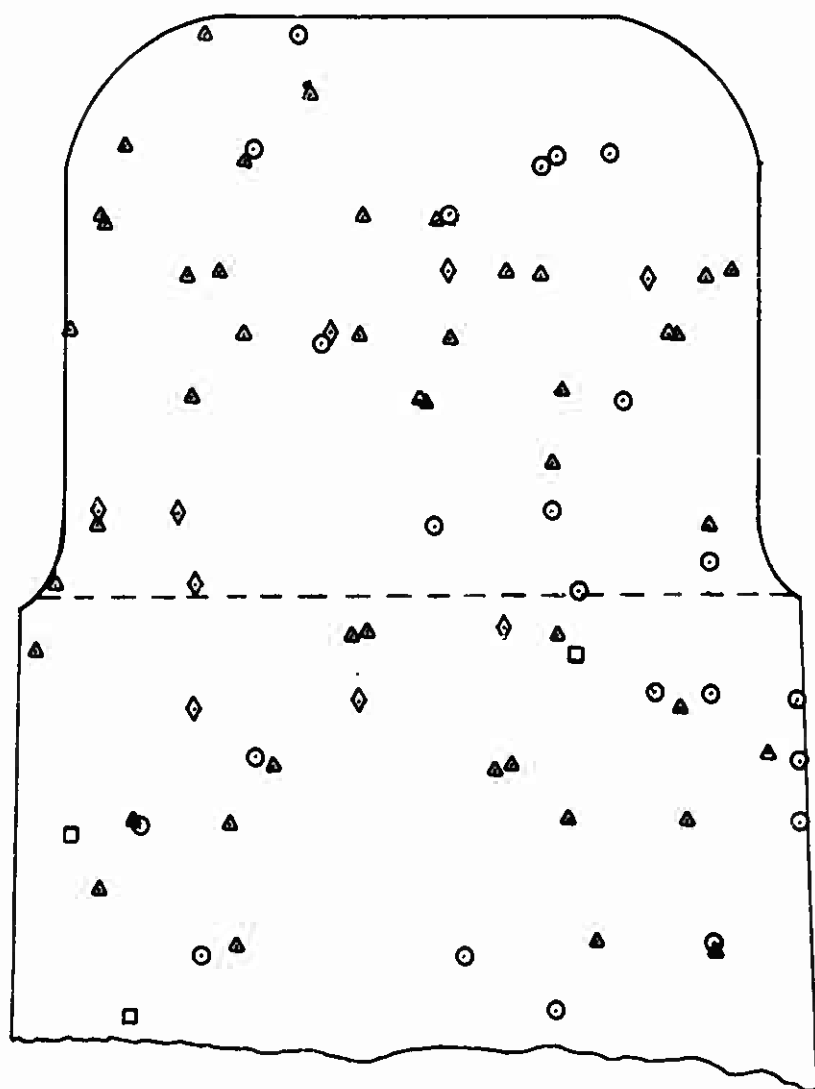
#### d. Discussion of Map Data

Examination of the map for the motor with a sealed bore (Figure 15) shows sites are randomly distributed throughout the propellant. In this case, with no diffusion gradients from the atmosphere available, it is concluded that components of the propellant formulation led to the formation of the reaction sites. Propellant samples that had surfaces exposed to the atmosphere (Figures 10 through 13) show a higher volume concentration of sites close to the exposed surfaces.

RELATIVE VOLUME CONCENTRATION OF REACTION SITES FOR  
A MODEL IGNITER GRAIN AGED FOR 3 MONTHS



DISTRIBUTION OF REFRACTIVE REACTION SITES IN SEALED  
IGNITER MOTOR, 3 MONTHS AT 125°F

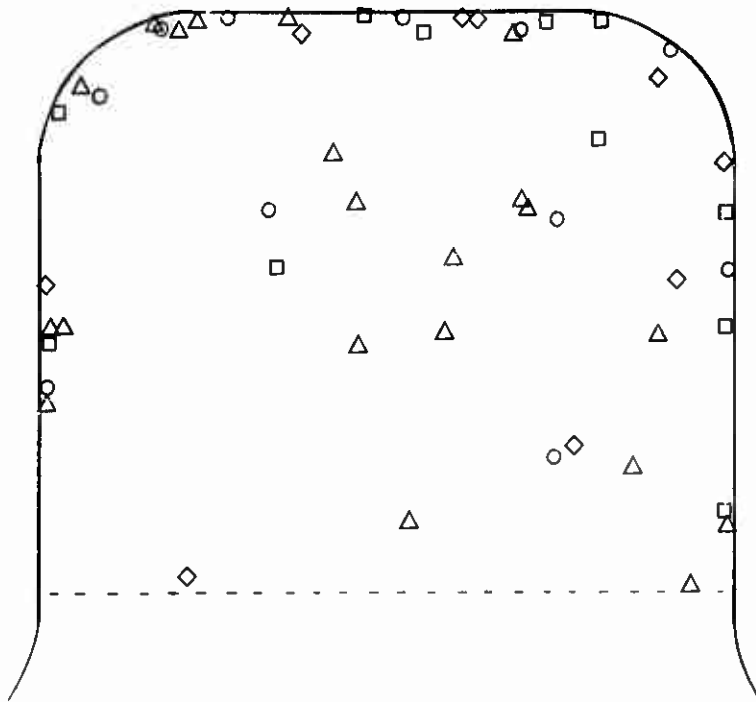


Size

Scale 10:1

- Δ ≤ .025 mm<sup>2</sup>
- ≤ .059 mm<sup>2</sup>
- ◊ ≤ .075 mm<sup>2</sup>
- ◻ ≤ .100 mm<sup>2</sup>

# DISTRIBUTION OF REFRACTIVE REACTION SITES IN FIELD IGNITER MOTOR, 1 YEAR OLD



Size

Scale 10:1

- $\Delta \leq .025 \text{ mm}^2$
- $\circ \leq .050 \text{ mm}^2$
- $\diamond \leq .075 \text{ mm}^2$
- $\square \leq .100 \text{ mm}^2$

FIGURE 16



There are two plausible explanations for this larger concentration of sites near the surface. The first is that atmospheric components (i.e. moisture and/or oxygen or other oxidizing species) are reactants in site formation and chemically react with propellant ingredients to increase site formation. A second possibility is that a concentration gradient exists in which mobile components (plasticizer, for example) in the propellant migrate towards the surface because of thermal and/or concentration gradients, and in this diffusion process carry along components (iron acetylacetonate and dissolved  $\text{NH}_4\text{ClO}_4$ ) that react to form sites. Data from this portion of the study did not provide information as to which of these pathways actually occurred.

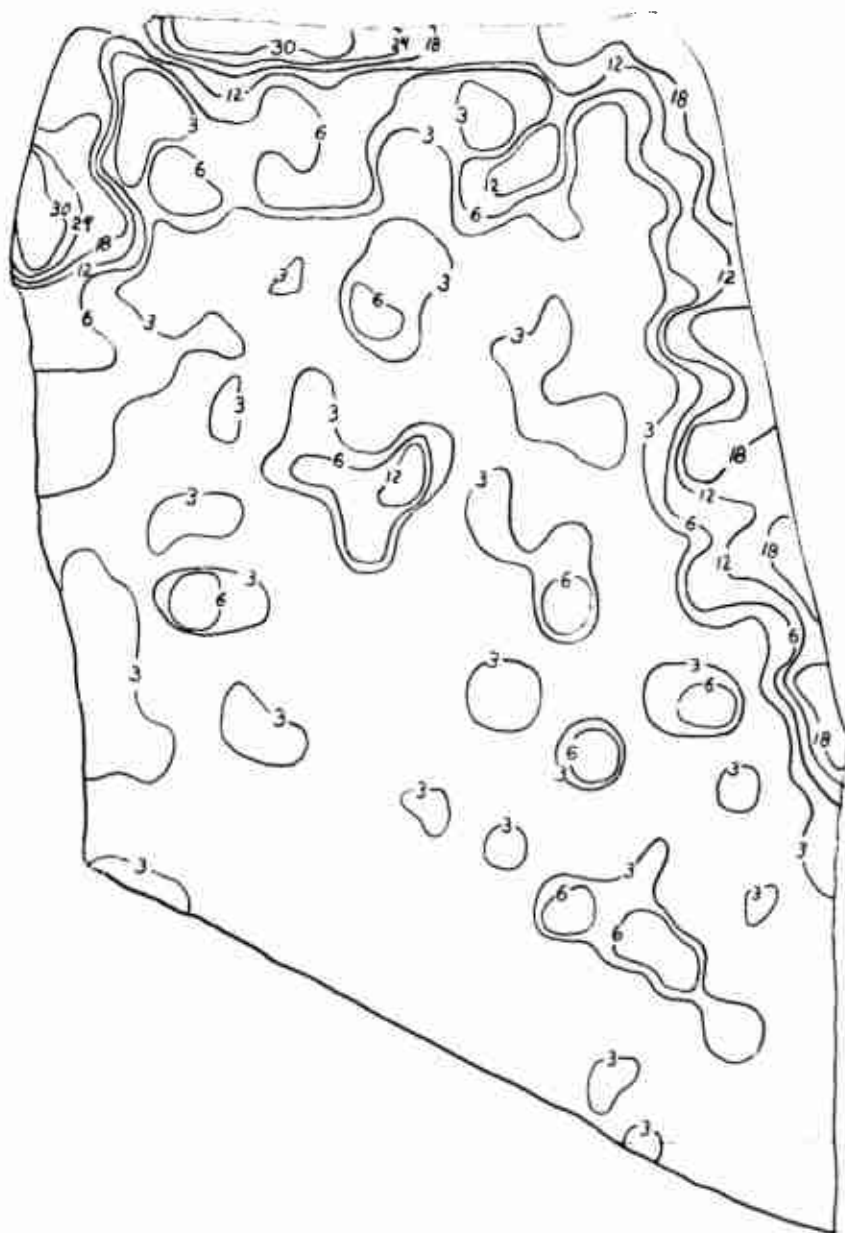
The decrease in the total volume of reaction sites as the storage temperature was increased showed that while overall binder degradation increases with temperature, the conditions for site formation are more favorable at a lower temperature. We postulate that this is due to the destruction of the reaction intermediates required to generate the reaction sites as the temperature is raised. In other words, at higher temperatures, the rate of formation of reaction sites is lower than the rate of destruction of the reaction intermediates required for site formation.

The possibility that the site formation was due to a volatile component which was eliminated at higher temperatures was dismissed. None of the propellant ingredients was sufficiently volatile and the reaction site formation was not greatly increased in the sealed motor where loss of material through volatility would not be a factor.

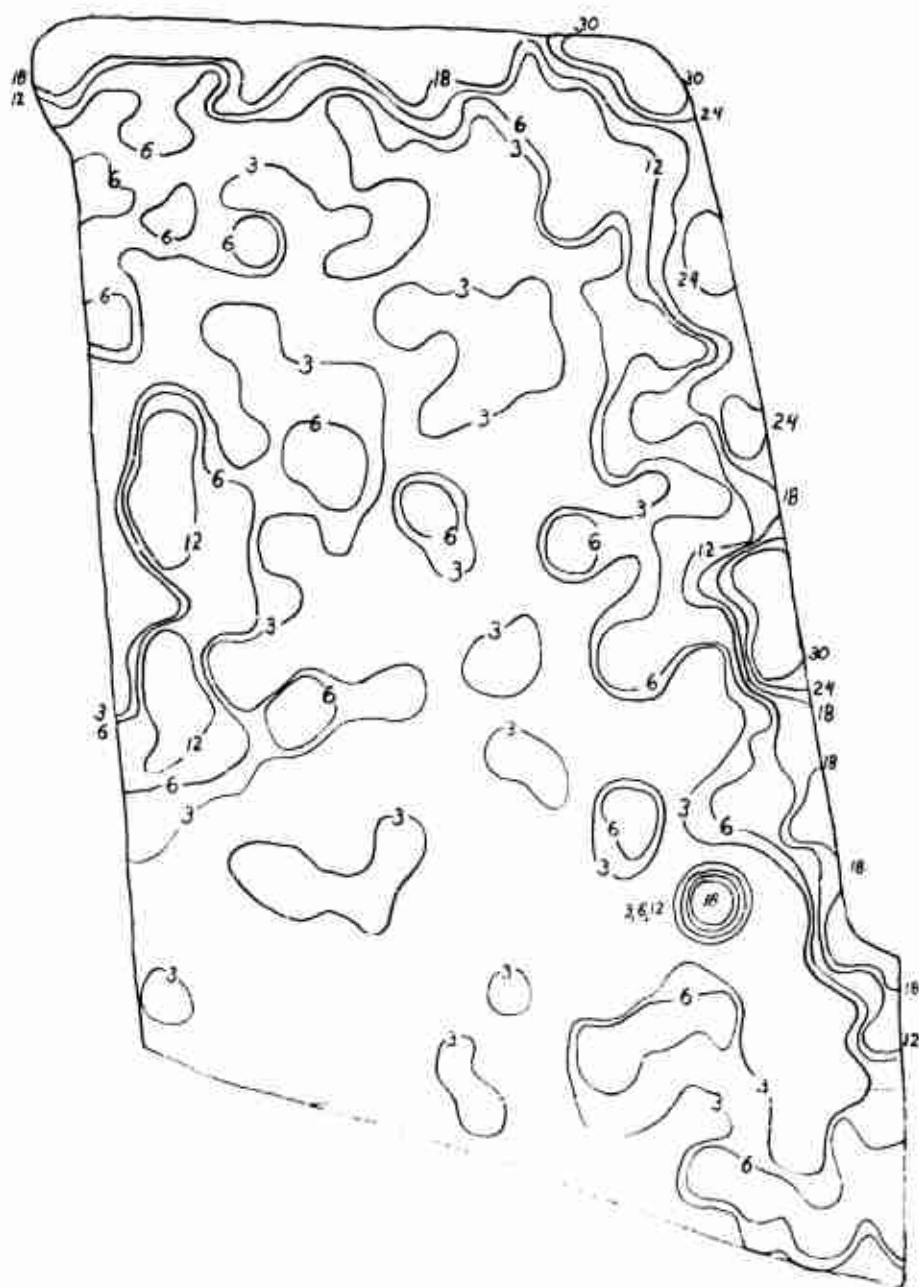
e. Planimetric Analysis of Refractive Sites in  
Model Igniter Grains Aged Six Months

The only change in the procedure was to maintain the isopleth interval a uniform 6% whereas the initial interval was 3%. The analysis of the six-month samples was limited to the ray tips. Figures 17 through 20 are isoplethic maps (relative volume concentration contours) which express the relative concentration gradients. The results of the planimetric analyses for the 3- and 6-month periods are shown in Table II and Figure 21. It is apparent that the formation or growth of refractive type reaction sites has continued during the 3- to 6-month interval, but at a reduced rate from the first three-month interval. The percent increase between the 3- and 6-month periods is shown in Figure 22. The lower position of the 120°F point reflects a possible retardation of the reaction by the 50°F storage for part of the interval (see Table II). At 110°F, the sites apparently double in volume every year. This rate of growth is too large to be maintained over a long period since these propellants show good long range stability. These rates must, therefore, be only temporary or initial rates.

ISOPLETH MAP, MODEL IGNITER GRAIN  
6 Months 110<sup>0</sup>F, A



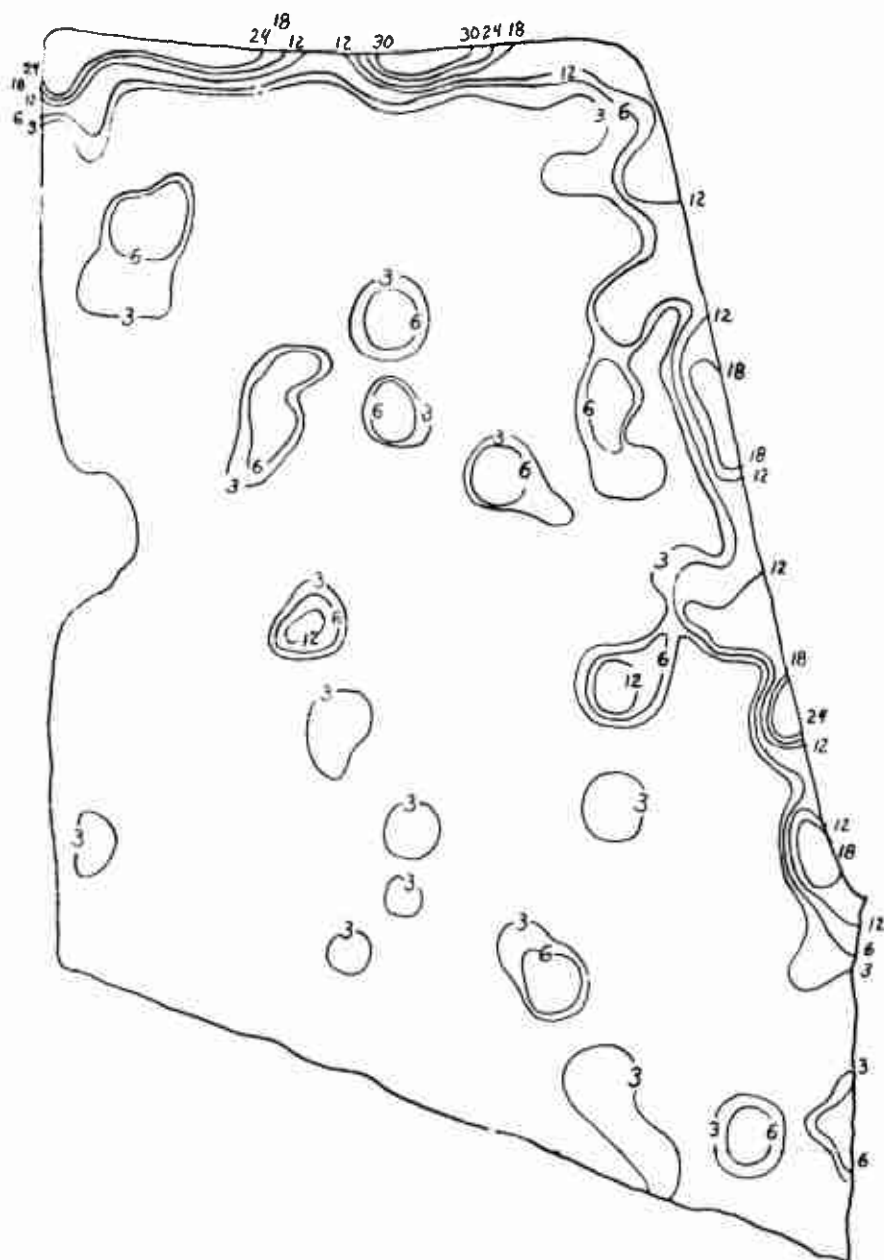
ISOPLETH MAP MODEL IGNITER GRAIN  
6 Months 110<sup>0</sup>F, B



ISOPLETH MAP, MODEL IGNITER GRAIN  
 3/3 Months 120/50°F, B



ISOPLETH MAP, MODEL IGNITER GRAIN  
6 Months 130<sup>0</sup>F, B



RELATIVE VOLUME CONCENTRATION OF REFRACTIVE SITES  
IN MODEL IGNITER GRAINS AGED 3 AND 6 MONTHS

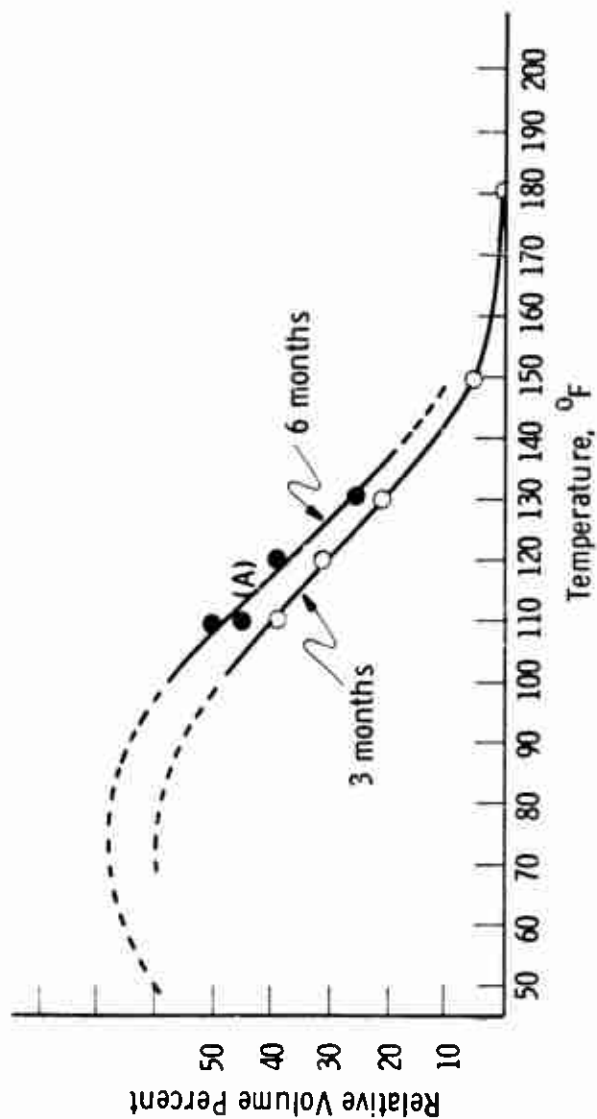


FIGURE 21

PERCENT INCREASE IN REACTION SITE VOLUME  
BETWEEN 3 AND 6 MONTHS SAMPLES

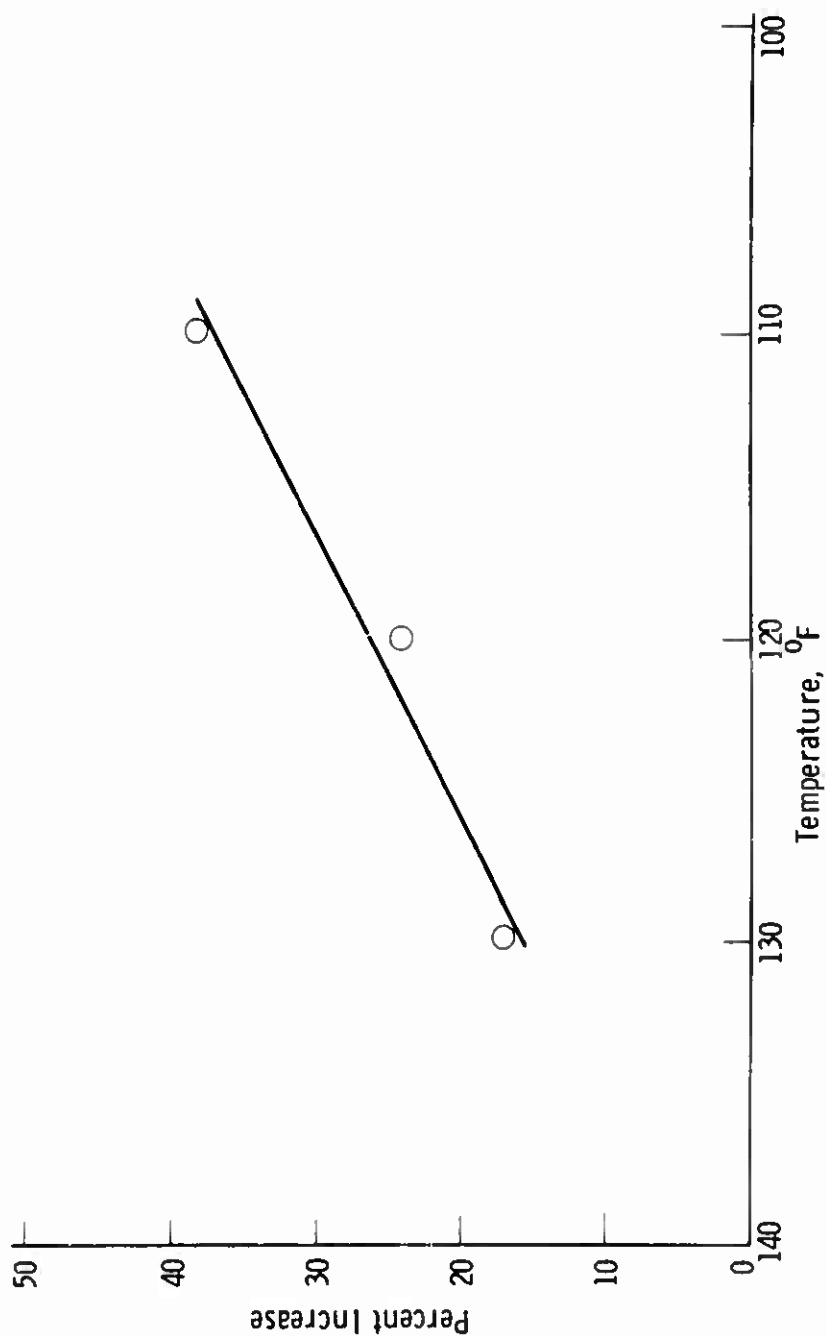


TABLE II  
RELATIVE VOLUME PERCENT OF REFRACTIVE SITES IN MODEL IGNITER  
AGED FOR 3 AND 6 MONTHS

Storage Temp. (°F)	Aging Time, months		Volume Increase, %	Rate of Increase %/yr
	3	6		
110		52.5	38.5	96
110	37.9	43.5		
120 <sup>a</sup>		38.9	24.3	61
120	31.3			
130		25.0	17.9	45
140	21.2			
150	5 <sup>b</sup>			
180	1 <sup>b</sup>			

<sup>a</sup> Stored at 120°F for 108 days, then kept at 50°F  
for remainder of study

<sup>b</sup> Estimated

#### f. Refractive Site Absolute Volume

The foregoing contour maps were drawn through points of equal refractive site concentration in which the concentration values were assigned on a relative basis. To obtain the real volume, the number and size range of particles in 0.25 square microns were determined, using the calibrated grid eyepiece in the microscope. The areas of all refractive sites were summed and divided by the total area of the mapped section, which was 1/100 the area obtained by a planimeter from the enlarged maps. The actual volume concentration was determined from the fact that the ratio of the areas of the parts to the total area was equal to the ratio of the volumes of parts to the total volume. The absolute and relative volume concentrations are listed in Table III.

TABLE III  
RELATIVE AND ABSOLUTE VOLUME CONCENTRATION  
OF REFRACTIVE SITES

Sample Age, months	3		6	
	110	130	110	130
Sample Temperature, °F				
Relative Volume, %	37.9	21.2	52.5	25.0
Absolute Volume, %	.845	.376	1.0	.51



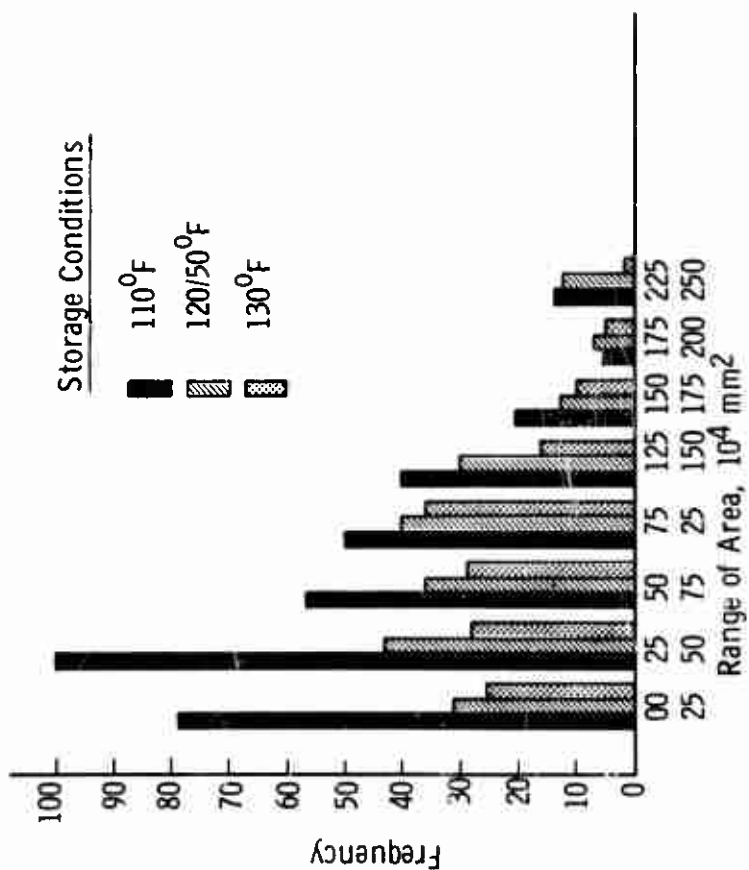
The accuracy of these values should be considered. The linear intercept technique has a maximum accuracy of  $\pm 1\%$  for each unit measured and the mapped value of  $1\%$  would be correct to  $1.00 \pm .01\%$ . This accuracy was demonstrated in work from this laboratory under The Sophy program (Final Report AFRPL-TR-67-211, Project Sophy Vol II, p 69, August 1967), where the volume of propellant voids was determined by the microscopic linear intercept technique and by a bulk liquid displacement technique. In reaction site measurements, the data were recorded by area and grouped in ranges of size. This caused a statistical error in the size distribution. Furthermore, the maximum accuracy is achieved only for particles of an ideal size, shape, and refractive index. The propellant voids in the Sophy program represented an ideal case while the refractive sites were not of ideal size, had variable refractive indices and were irregular in shape. The irregular shapes were in fact the reason for preferring the area measurement method to a linear intercept method. The area measurement method also gives an accuracy of  $\pm 1\%$ . Incidentally, recent literature has shown that a point counting technique may be preferable to both in accuracy and speed of operation.

#### g. Size Distribution

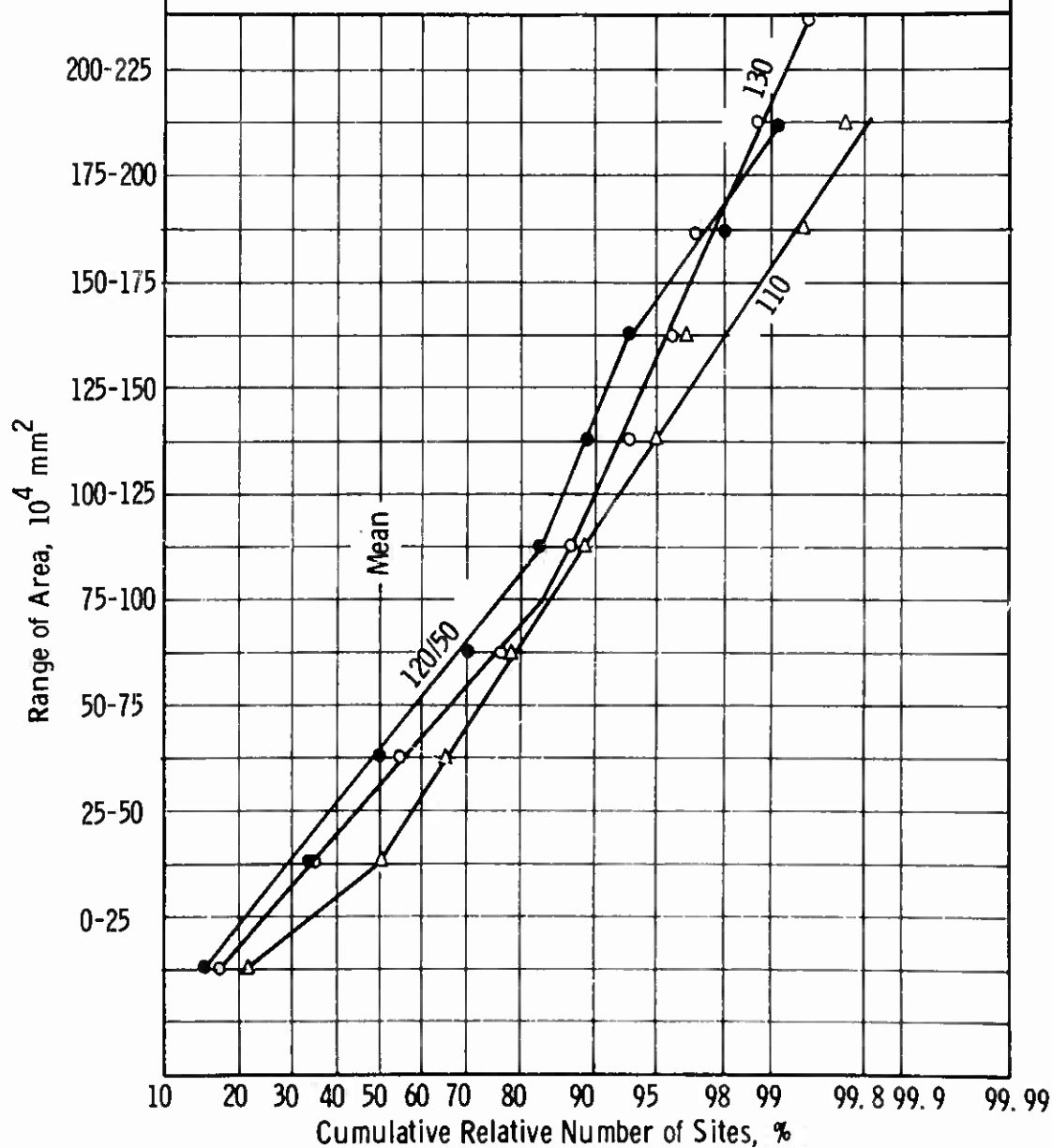
Size distribution of the refractive sites was statistically evaluated in order to determine the relation between frequency and size. The data are presented for samples aged six months; as a histogram, Figure 23, and as a probability chart, Figure 24. The histogram indicates the greatest frequency of reaction sites occurred at  $110^\circ\text{F}$  and progressively decreased as the temperature increased. With increase in temperature, the size of the most frequently occurring site increased; from  $.0038 \text{ mm}^2$  at  $110^\circ\text{F}$  to  $0.01 \text{ mm}^2$  at  $130^\circ\text{F}$ . Also, as shown on the probability plot, the mean particle size is least for the grain aged at  $110^\circ\text{F}$ . There are more small refractive sites per unit volume at the lower temperature; that is, nucleation was faster at  $110^\circ\text{F}$  while growth was faster at  $130^\circ\text{F}$ . This line of reasoning holds for the sample aged at  $110^\circ\text{F}$  which has nearly Gaussian population distribution (straight line probability plot). A break in slope of the sample aged at  $130^\circ\text{F}$  indicates that there was an increase in the rate of growth relative to the nucleation rate after a size of  $.0075$  to  $.0100 \text{ mm}^2$  was attained.

The probability line for the sample cycled from  $120^\circ$  to  $50^\circ\text{F}$  has a double break in slope. If this is interpreted as indicative of a bimodal distribution, then there is the probability of a second generation nucleation step due to the temperature cycle. Since this line is higher at the mean position, the reaction sites have grown larger than in either of the grains kept at constant temperature. This grain was cycled to evaluate field conditions and it is evident that even a single cooling cycle does modify the aging characteristics.

# HISTOGRAM OF REFRACTIVE SITE SIZE IN MODEL IGNITER GRAINS AGED 6 MONTHS



# PROBABILITY PLOT OF REFRACTIVE SITE SIZE IN MODEL IGNITER GRAIN AGED 6 MONTHS



## 2. Color Type Reaction Sites

### a. Description of Sites in Field Aged Motor

Colored reaction sites were detected in Hawk motors which at the time of initial microscopic examination had been aged for 4-1/2 years. Optical characterization of the reaction sites gave the following data (Figure 25-a - d). The colored reaction site photographed in transmitted white light had an absorption halo caused by fine particles suspended in the binder around a central aluminum particle. In doubly polarized light, the absorption was less birefringent, due to blacking of the light by suspended particles and the loss of birefringent material. When the same area was viewed by dark field phase contrast, blue light was seen to form a shell around the colored reaction site.

The ring of blue light observed by dark field phase illumination has not been reported in the periodical literature reviewed, nor in any standard text book. The color of the light is specifically a sky blue. The color is uniform and does not depend upon its position relative to the position or number of the Liesegang ring; nor does it depend upon the absorption color or the location in the propellant of the reduction site. These facts suggest a form of Rayleigh scattering which gives the sky blue color.

Further, in dark field phase contrast optics, light must be diffracted or bent to enter the objective. Any particle with a thickness and refractive index capable of bending the light sufficiently to enter the objective should be observed as a discrete particle. Since no such particles were observed, the bending was not the result of refraction of the light. The only other mechanism for bending the light was scattering by very small particles.

Discrete particles were not observed at the point source of the blue light in either plane or doubly polarized light. Inasmuch as the microscope has a resolution limit of 300 millimicrons and a detection limit of 50 millimicrons, the particles causing the light scattering must be of molecular size. Therefore, it is concluded that the blue light is a form of Rayleigh scattering by molecular size particles.

In the Hawk field motors, a radial color gradient from red-orange near the bipropellant interface to the blue-green near the bore surface was observed at the 4-1/2-year period, Figure 26 (left). The color gradient, due to iron in different oxidation states, was indicative of a reducing environment in the booster propellant. At the end of 5-1/2 years, the color rings had developed characteristic black shells indicating further reduction of the iron compounds.

# LIGHT SCATTERING AROUND COLORED REACTION SITES



-pol

a



+pol

b



d. f. phase

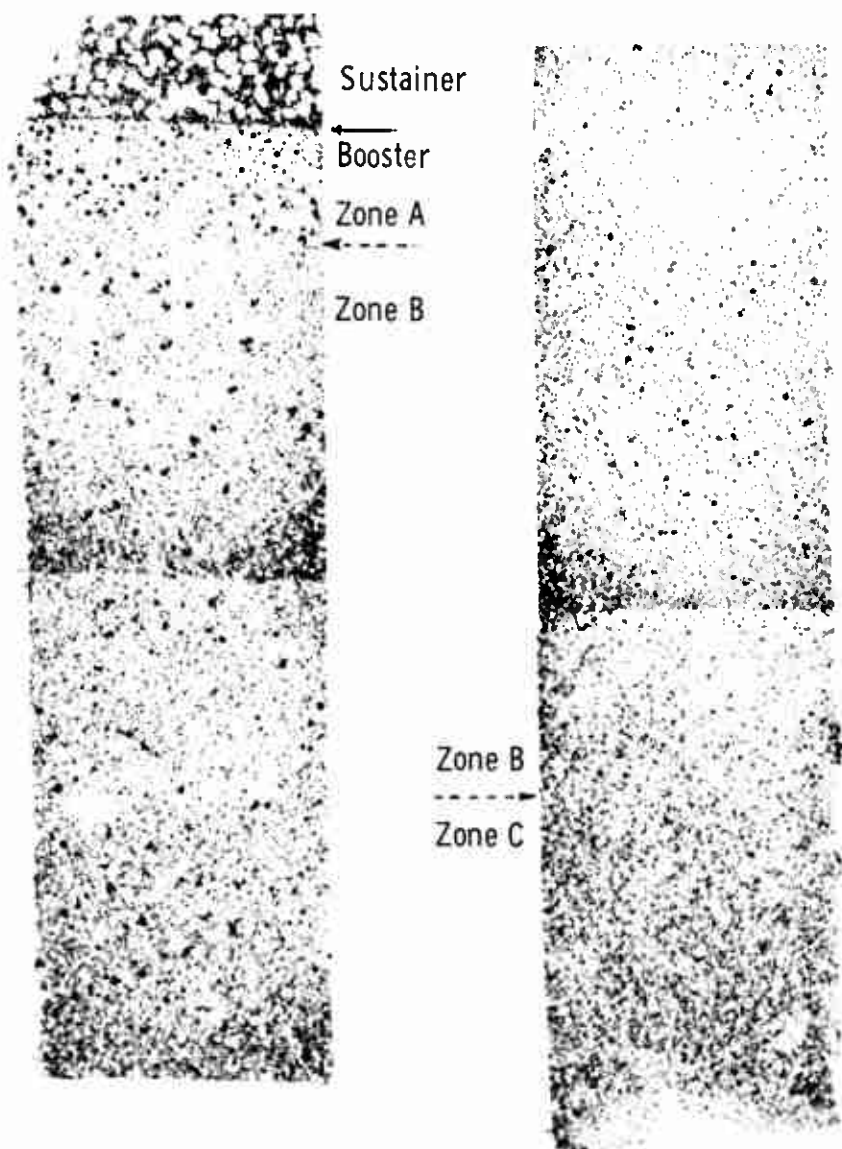
c



d. f. phase + blue filter

d

HAWK FIELD MOTOR, 5-1/2 YRS, DISTRIBUTION OF  
COLORED REACTION SITES AT FORWARD END



Magnification 6X

Ray Surface

In Figure 27-c, a large central aluminum particle is surrounded by a diffuse, deep gray-green color caused by submicroscopic particles in the binder. The halo has the normal birefringence caused by the contained microatomized  $\text{NH}_4\text{ClO}_4$ . There is no indication of conversion of  $\text{NH}_4\text{ClO}_4$  to  $\text{NH}_4\text{Cl}$ , nor is there any of the altered refractive index material. In Figure 27-d, a bright altered refractive index center is enclosed by several opaque particles, which are in turn surrounded by a colored halo. This halo is composed of many translucent green-brown particles with a uniform size of about one micron. This same type of halo is more frequently observed around large single aluminum particles. The central collection of opaque particles lacks the reflectivity of the aluminum and was not further identified.

The precipitation into the colored rings was the result of the reduction of the iron acetylacetonate. Zone A (Figure 26) has been influenced by the proximity of the adjacent sustainer, which contains more FeAA than the booster. Apparently, there has been bulk migration of iron across the bipropellant interface creating Zone A. Evidence for this migration is presented in Section II.C.2.b. and 3. The high frequency and small size of sites in Zone C near the propellant surface represents a high rate of site formation with a slow rate of growth. Possibly Zone C nearer the bore surface was more completely exposed to maximum thermal cycling (heat flow) with thermal gradients decreasing toward the B/C Zone line. Zone B was exposed to a relatively more constant thermal environment with the most thermally stable environment near the B/A Zone line.

A batch of propellant with the Hawk formulation was made and studied at shorter time intervals to follow the color site formation.

#### b. Colored Reaction Sites in Model Bipropellant Grains

Colored reaction sites appeared in the sample aged 3 months as a gray-green diffuse precipitate; after 6 months of aging they were found throughout most of the ray section and were partially condensed into definite Liesegang ring (actually shells) structures. In the 9-month sample the red gel center, similar to those in the 4-1/2 and 5-1/2 year old Hawk motors, was observed. Size, a recorded characteristic in the case of refractive sites, was not recorded for the colored sites because a straightforward volumetric relationship was lacking. The diffuse boundary between the colored and non-colored zone rendered size measurements between samples of different ages uncertain, but a microscopic frequency plot of the colored reaction sites was prepared and an isopleth map was constructed. The schematic map in Figure 28 illustrates the general distribution of refractive and colored reaction sites in a small 6- to 9-month old bipropellant grain stored at 120°F.

REACTION SITES, REFRACTIVE AND COLORED TYPES  
(320X)



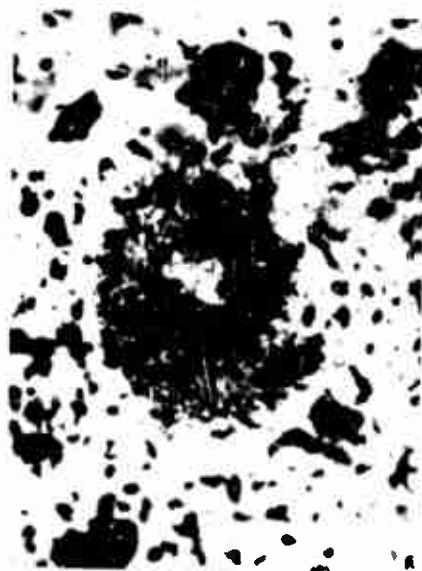
a



b



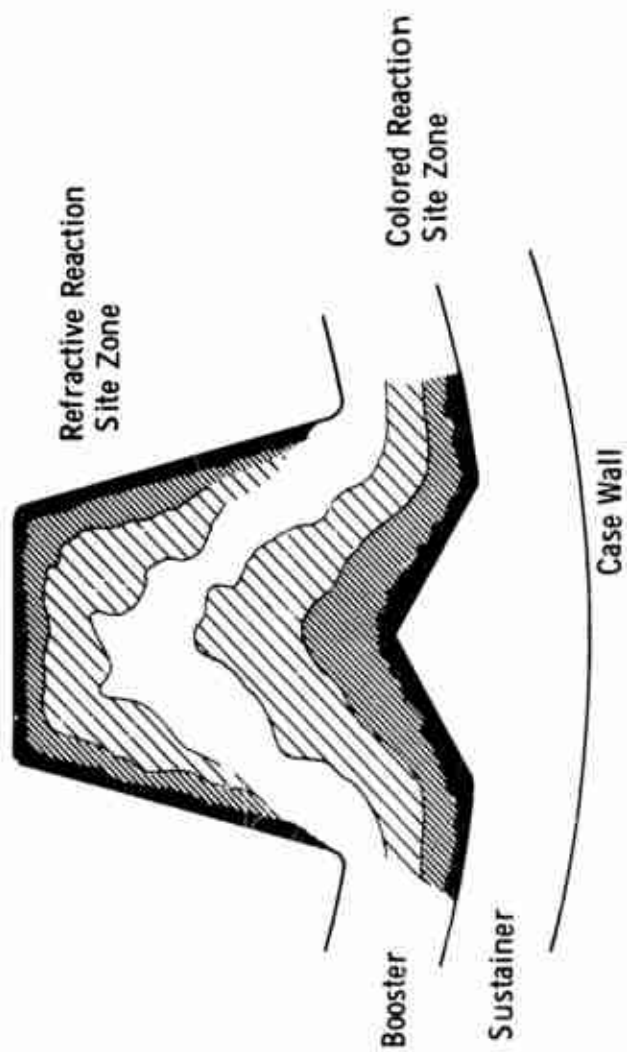
c



d



SCHEMATIC ISOPLETH MAP SHOWING LOCATION OF COLORED  
AND REFRACTIVE REACTION SITES IN A BI-PROPELLANT CROSS SECTION



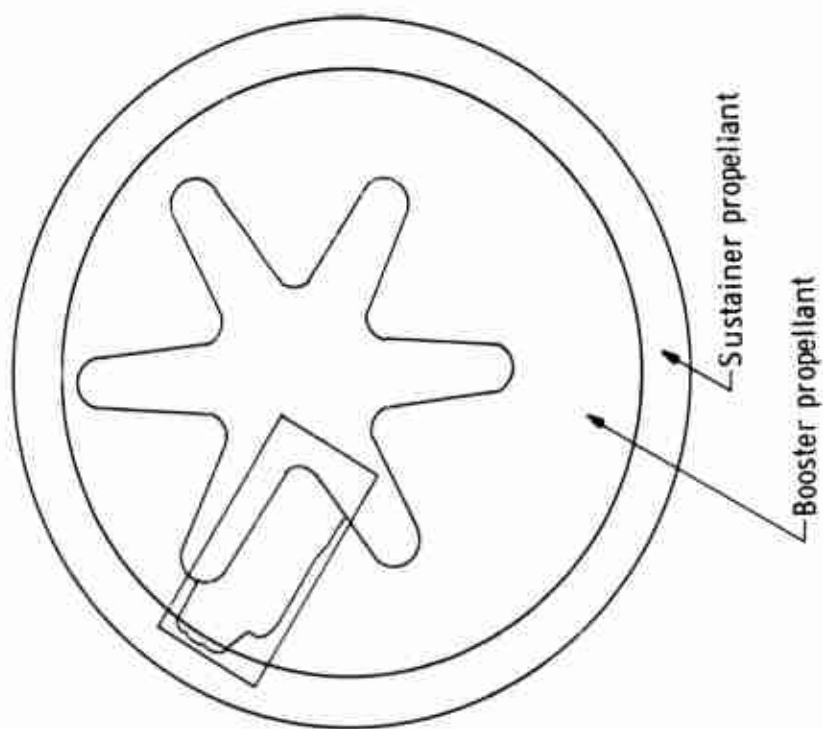
A thin section from the model bipropellant grain aged 9 months was selected for study. A preliminary examination was made to determine the characteristics to be recorded. The chief characteristic was color, but establishing color standards for classifying the sites was complicated by the fact that different rings in these reaction sites (composed of concentric shells) have different colors. After review of samples from grains of other ages, including Hawk propellants, a system of gross color characteristics was selected for classifying the colored sites.

The microscopic procedure followed the technique developed for measuring concentration gradients in the case of refractive type sites. Because the concentration of colored sites is greater than that of the refractive sites, a satisfactory statistical sampling for a given area of sample was achieved by studying every fourth site. The data was plotted on a ten-fold enlarged drawing of the ray cross section. (The maps of the igniter and bipropellant grains are similarly enlarged.) The location of the mapped section relative to the grain geometry is shown in Figure 29. A 0.25 centimeter grid was laid over the plotting sheet and covered by a sheet of vellum. A one centimeter circle was again used for the countout on a quarter centimeter grid. The numbers recorded are  $1/4$  the frequency of occurrence of colored reaction sites, and the labelled values multiplied by 4 give the actual frequency. Maps were made on the basis of a number of different color classification schemes. The first map, Figure 30, shows the frequency of all colored reaction sites. Sites of a clear yellow-green stain are mapped in Figure 31; those characterized by a green refractive gel are mapped in Figure 32; sites with a green stain plus a red-orange stain, in Figure 33; and those showing a red-orange gel plus a green-brown stain, in Figure 34.

The data were contoured to better show the concentration gradients. Observation showed that symmetry exists about a center line bisecting the ray, and therefore, the grain geometry controls the distribution of sites. Note that the left side of the map at the base of the ray is a bipropellant interface and that a contour high, i.e., a reaction site concentration maximum, occurs about a centimeter into the ray and parallel to the bipropellant interface. Figures 31 through 34 show a progressive color change from the bipropellant interface to the bore surface.

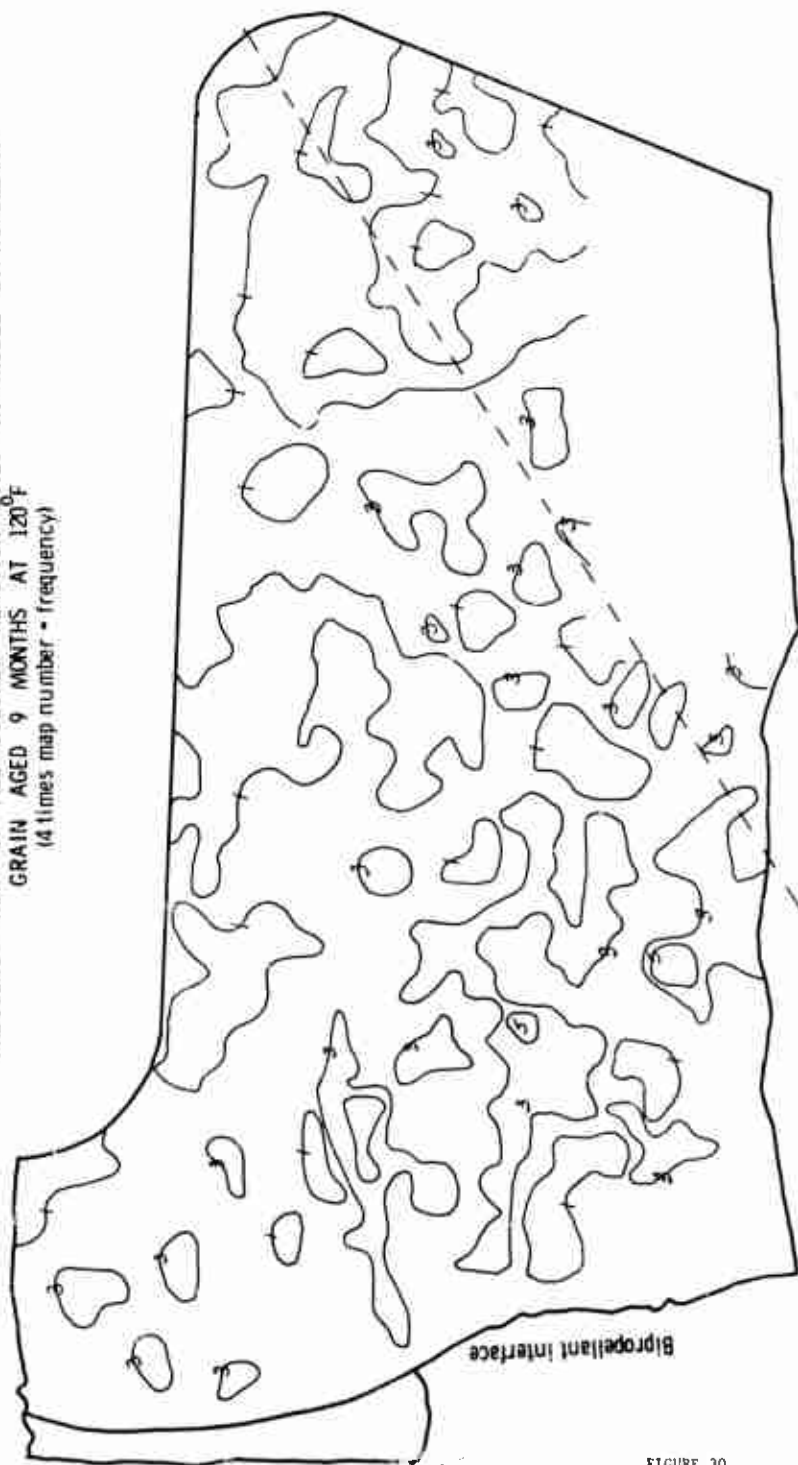
The mapped data showed that color sites in the model motor were uniformly distributed in the booster segment, rather than being localized near the bipropellant interface as in the case of the field motor. The data of the model grain was obtained for 9 months storage at 120°F as compared to the 4-1/2 year storage of the field motor, and this supports the conclusion that site formation is a random process and that thermal and diffusion gradients are not needed to initiate site formation. However, on storage, diffusion and thermal gradients led to migration of species which resulted in a higher frequency of color sites near the bipropellant interface. The identity of these migrating species was established by chemical analysis as described in Section II.C. to be plasticizer and FeAA.

CROSS SECTION OF MODEL BI-PROPELLANT GRAIN  
SHOWING LOCATION OF MAPPED AREA



Scale 1:1  
Dia. 4-3/4

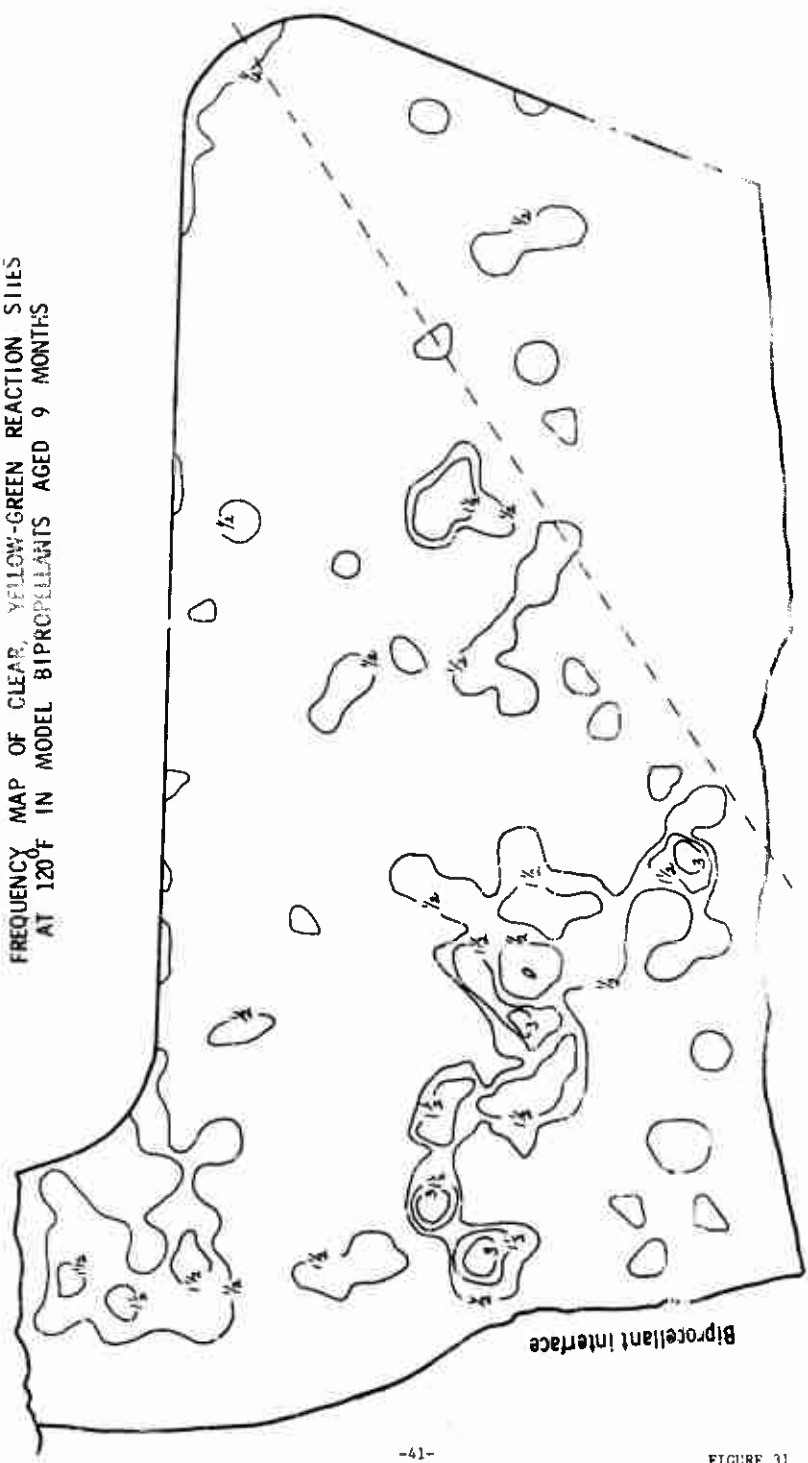
FREQUENCY MAP OF ALL COLORED REACTION SITES IN MODEL BIPOPELLANT  
GRAIN AGED 9 MONTHS AT 120°F  
(4 times map number • frequency)



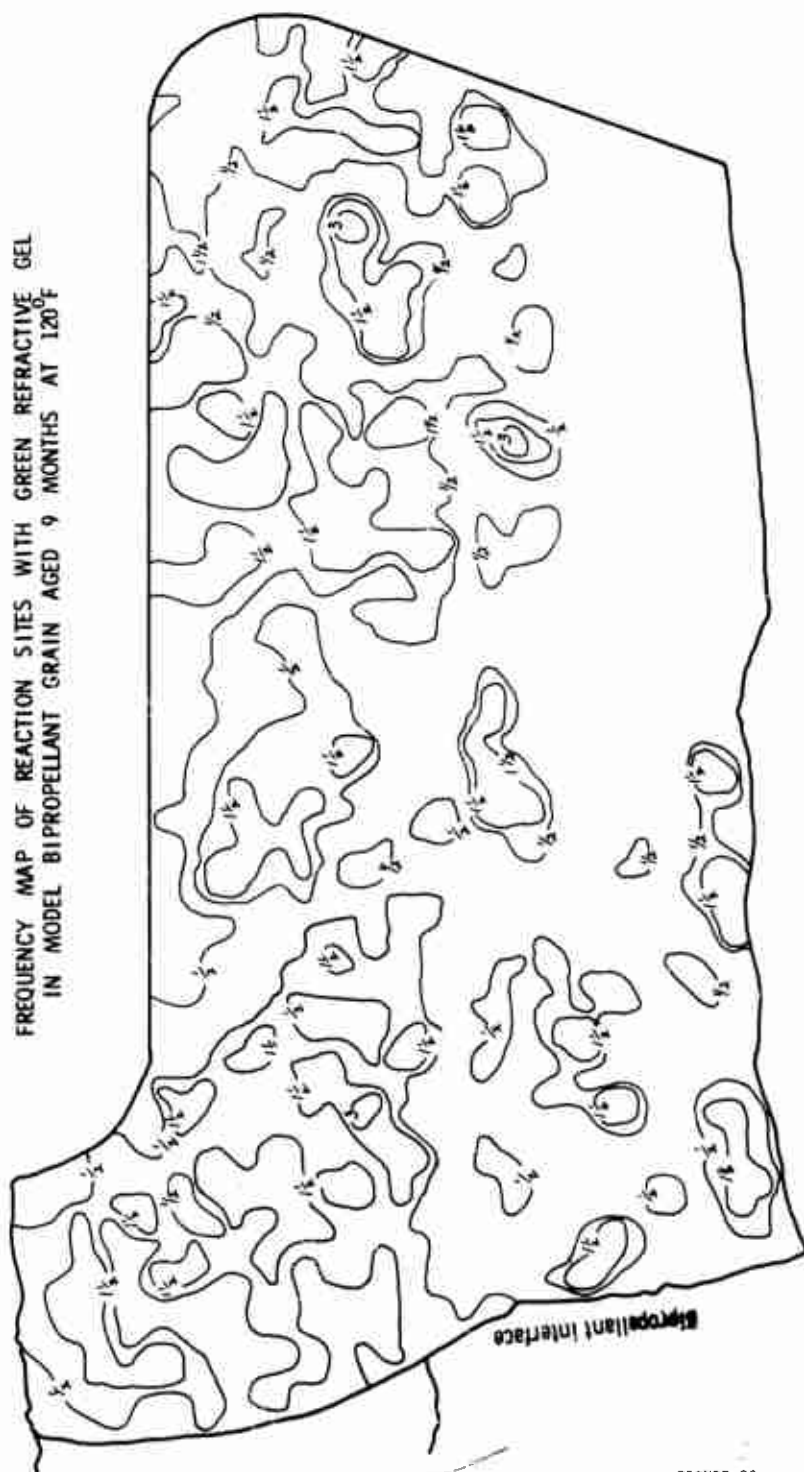
-45-

FIGURE 30

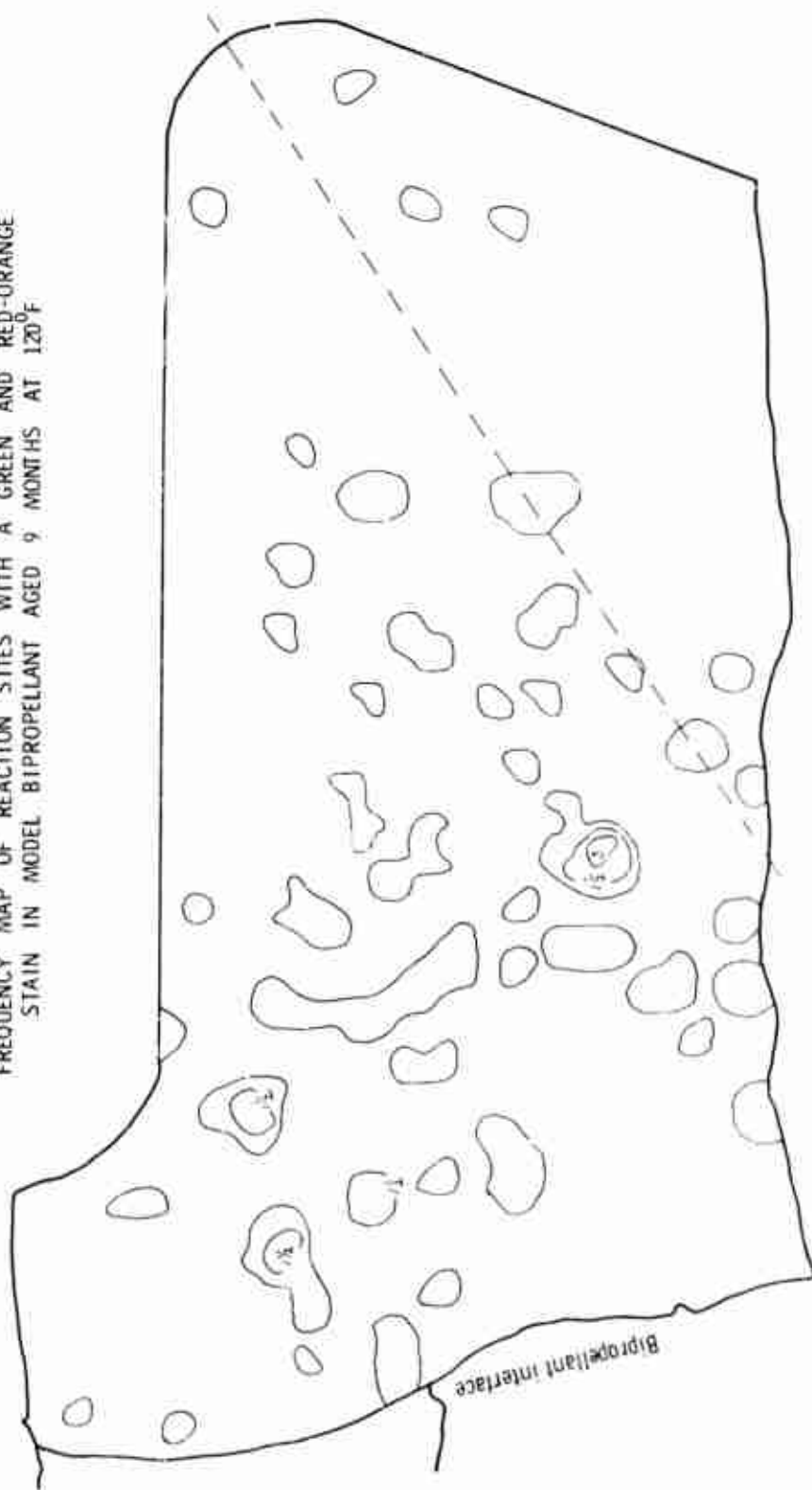
FREQUENCY MAP OF CLEAR, YELLOW-GREEN REACTION SITES  
AT 120°F IN MODEL BIPOCELLANTS AGED 9 MONTHS



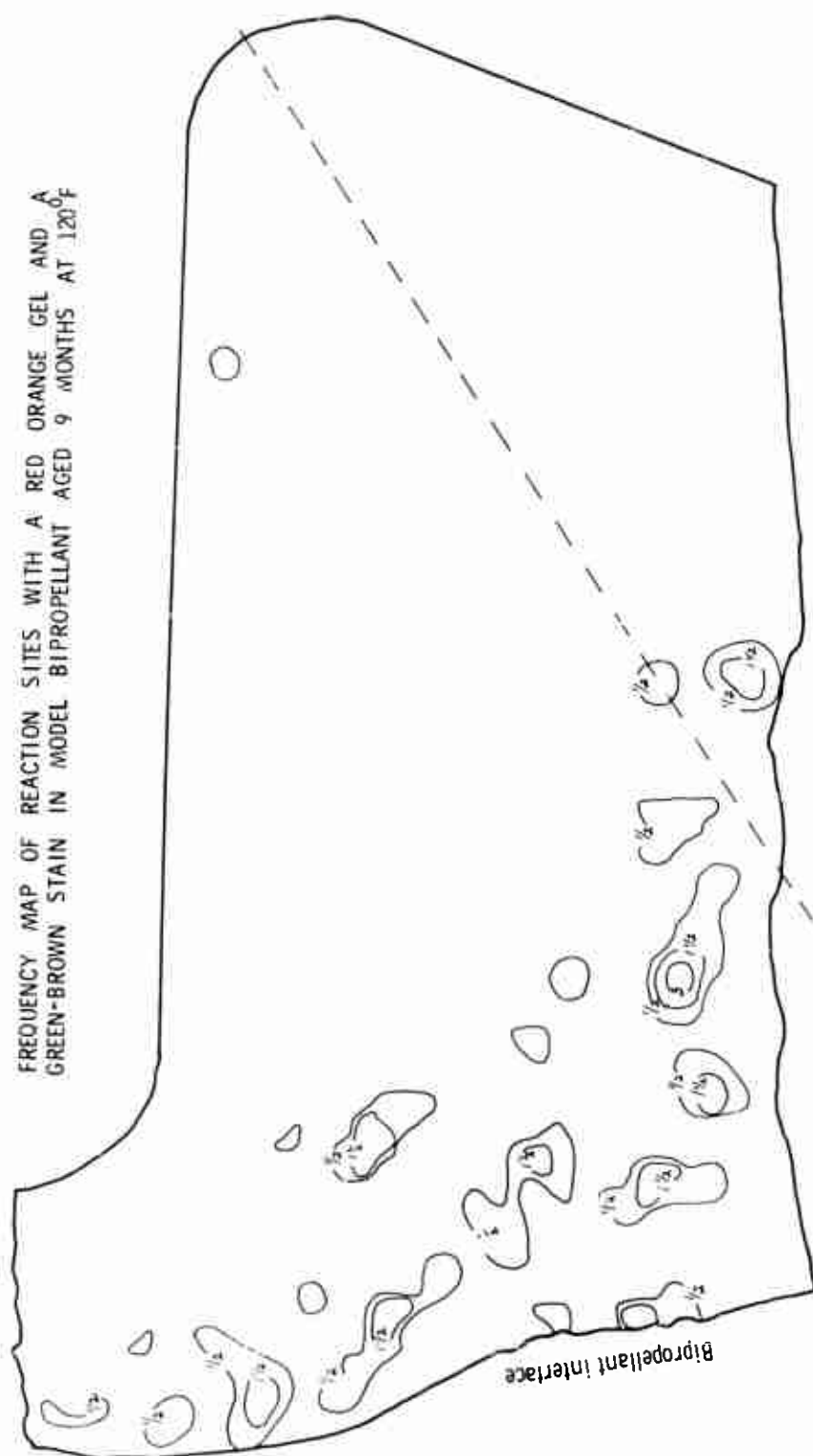
FREQUENCY MAP OF REACTION SITES WITH GREEN REFRACTIVE GEL  
IN MODEL BI-PROPELLANT GRAIN AGED 9 MONTHS AT 120°F



FREQUENCY MAP OF REACTION SITES WITH A GREEN AND RED-ORANGE  
STAIN IN MODEL BIROPELLANT AGED 9 MONTHS AT 120°F



FREQUENCY MAP OF REACTION SITES WITH A RED ORANGE GEL AND A  
GREEN-BROWN STAIN IN MODEL BIROPELLANT AGED 9 MONTHS AT 120°F





### 3. Conclusions from Microscopic Studies

The frequency, concentration, and size distribution of reaction sites in model grains of Minuteman igniter propellant were derived. These showed that in model grains the formation of reaction sites was greater at 110°F than at 180°F. From the fact that the size of the most frequently occurring site increased as the temperature increased, it was concluded that the growth of the sites was favored by higher temperature. Thus there were two factors; a nucleation or generation favored by low temperature, and a growth favored by high temperature.

The generation of sites occurred in random fashion and involved the propellant components without the need of material intruding from the environment. This fact was indicated by the random distribution of sites observed in a sealed propellant grain. However, intrusions from the environment and migration of propellant components significantly affects the reaction site formation. Under these conditions, the aging sites became concentrated at the propellant surface and at bipropellant interfaces.

The influence of the environment is assumed to be the result of moisture and air diffusing into the propellant. The migrating propellant components were iron acetylacetonate which was identified microscopically by the colors of the sites and chemically as described in Section II, and plasticizer identified chemically. Ammonium perchlorate may also migrate dissolved in the plasticizer. It has been observed deposited on the surface of aged Hawk grains examined under other programs. The migration is the result of concentration gradients, as in bipropellants of different composition, and thermal gradients which in field-stored motors result from exposure to daily temperature fluctuations.

The colors of the reaction site indicate that iron acetylacetonate is involved and that the iron exists in valence states ranging from 0 (black) to III (red). Because all reaction sites involve a core of aluminum metal, the aluminum is the reducing agent for the iron. No reaction sites are observed in non-aluminized propellants. The binder is also involved as indicated by the chemical studies described in the following sections.

The kinetics of reaction site formation were not adequately determined. In model Minuteman igniter grain the reaction site volume (about 1% at 6 months) increased at a rate of almost 100% per year at 110°F. Because this propellant is a rather stable one, it was concluded that the rate was a temporary or initial rate. Also, the accelerated aging of models may not be typical of field aged motors. In field-stored Hawk grains, aging sites are barely discernible at 3.5 years.

## II. CHEMICAL STUDIES

### A. INTRODUCTION

The microscopic observations that reaction sites were related to propellant aging prompted attempts to establish a chemical basis for the aging process. For this, it was necessary to identify the chemical compounds required to form the reaction sites. The first step in this process was to analyze the chemical composition of an aged propellant containing reaction sites.

### B. CHEMICAL ANALYSIS OF POLARIS CYCLING UNIT

A sample of degraded Polaris propellant which had been field aged for 7-1/2 years was chosen for initial chemical analysis. This sample contained a bore surface zone about 3/4 in. thick in which the binder network was degraded, plus a high concentration of refractive type reaction sites. The sites found in this propellant were identical with respect to optical microscopic properties with the reaction sites found in Minuteman Igniter propellant. The method used for analysis of this Polaris propellant was to separate the refractive sites from the degraded binder and to analyze separately each fraction. A 100-g sample of the degraded zone was mixed with 750 ml. of ethylene dichloride (EDC) to dissolve out the binder, leaving behind  $\text{NH}_4\text{ClO}_4$ , Al, and reaction site clusters. The ethylene dichloride will be discussed in the next section.

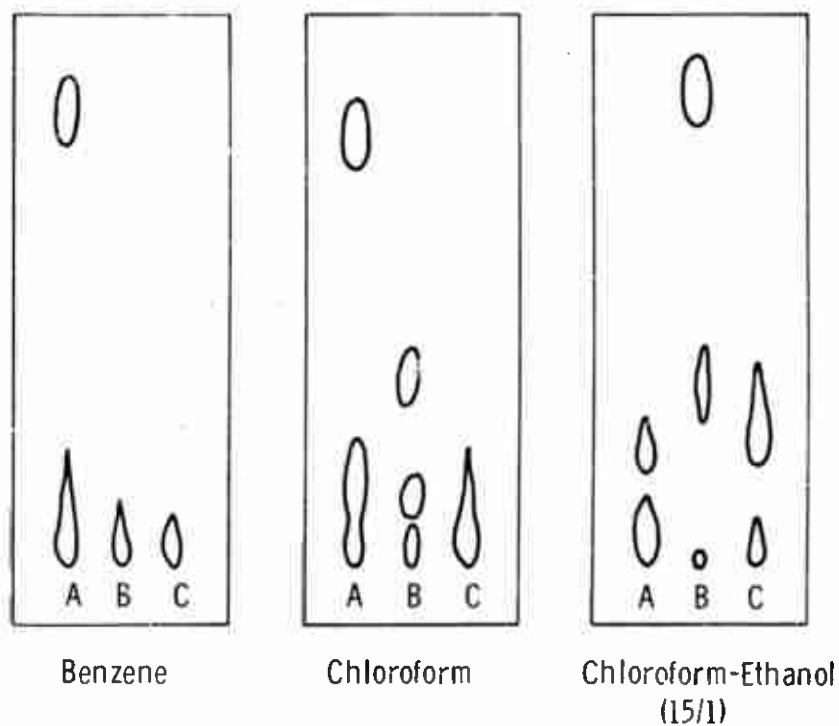
#### 1. Analysis of the EDC Soluble Fraction

A 2.8 g sample of degraded binder from the ethylene dichloride soluble fraction was placed upon an 18 mm x 75 cm alumina column and successively diluted with 300 ml portions of benzene, diethyl ether, and methanol. Evaporation of the eluents gave, respectively: Fraction A, 300 mg; Fraction B, 300 mg; and Fraction C, 900 mg. Each of these fractions was redissolved in 10 ml. of benzene and the solution used for thin-layer chromatographic analysis.

Silica-gel coated plates were spotted with about 2  $\mu\text{l}$  ( $2 \times 10^{-3}$  ml) of the test solutions. This volume is equivalent to about 0.06 mg of Fractions A and B, and 0.18 mg of Fraction C. The spotted plates were developed in separate chambers containing various solvents. The most informative chromatograms are shown in Figure 35. There are at least three components in A and B and two in C. The position of the spots indicate that some of the compounds are in more than one fraction. Similar TLC analysis with aluminum (basic) coated plates showed that the spots were more mobile than with silica gel (acidic), demonstrating that the components were basic.

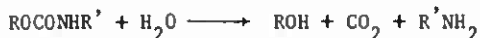
A more quantitative analysis of the soluble fraction was attempted by gas chromatography. A sample was injected into a chromatograph and passed through a 2-ft column containing a non-polar silicone coated support which was heated at a constant rate to 300°C. No detectable amount of material passed through the column showing that the molecular weights of the degraded fragments were too large for gas chromatography.

# THIN-LAYER SILICA-GEL CHROMATOGRAPHS OF DEGRADED PROPELLANT (See Text) FRACTIONS



A soluble fraction from a sample of the non-degraded binder was also examined by thin-layer chromatography. The mobility of the mixture from the non-degraded binder was lower than that of the mixture from the degraded portion, showing that the average molecular weight of the fragments in the degraded binder was lower. The infrared spectra (Figure 36) of the various fractions from either the degraded or non-degraded binder are identical and superimposable upon a spectrum typical for a polyurethane (Figure 37). The only difference between the degraded and non-degraded sections was the larger size of the polyurethane fragments in the non-degraded section of propellants.

Apparently then the degraded and non-degraded propellant consists of fragments of polyurethane split from the network. The polyurethane differed only in being of lower average molecular weight in the degraded propellant. The basic character of these polymer fragments suggests the presence of amino groups. These may arise from hydrolysis of a urethane as



or they may be due to N-(2-hydroxyethyl)-N,N',N'-tri(2-hydroxypropyl) ethylene-diamine used as a crosslinker in the Polaris propellant. Most likely is that the basicity arises from both sources.

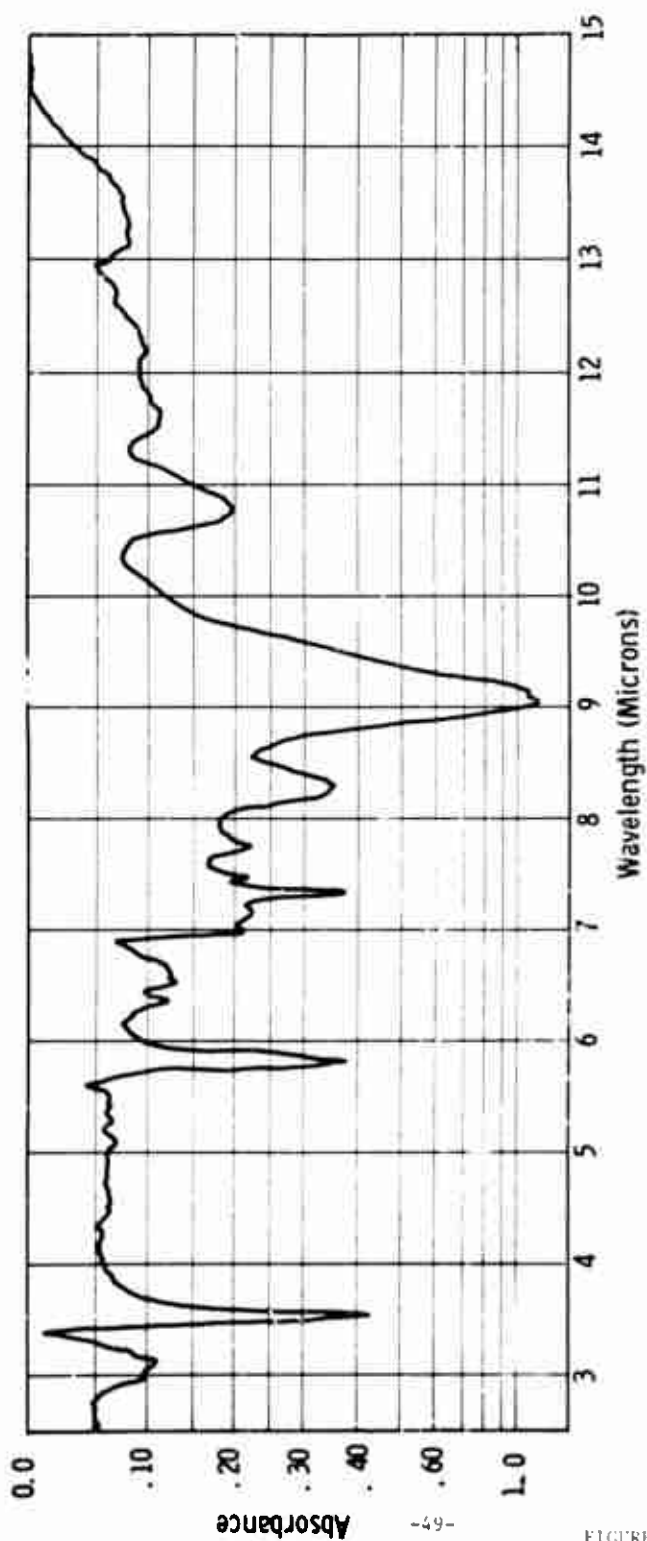
## 2. Analysis of the Polaris Refractive Sites

The slurry of  $\text{NH}_4\text{ClO}_4$ , Al and refractive site clusters was treated with dimethylformamide, which dissolved the  $\text{NH}_4\text{ClO}_4$ , leaving only Al and the reaction site clusters. This mixture was passed through a screen of appropriate mesh to separate the smaller Al from the reaction site clusters. Figures 38a to d show, respectively; (a) a typical reaction site in a thin section of propellant from a degraded zone; (b) four reaction sites isolated by ethylene dichloride, and contaminated with some  $\text{NH}_4\text{ClO}_4$ ; (c) a reaction site leached with dimethylformamide to remove  $\text{NH}_4\text{ClO}_4$ ; (d) a fragmented particle which originally was part of a reaction site cluster.

This clear material (Figure 38d) was insoluble in hot polar solvents as dimethylformamide, dimethyl sulfoxide and water, as well as common organic solvents. It was yellow-green, isotropic, non-birefringent and amorphous, with a refractive index of  $1.53 \pm 0.02$ .

An 0.6-g sample of air dried reaction sites, freed from ammonium perchlorate, was shaken with 25 ml of 3N HCl for 4 hours to dissolve aluminum from the test sample. This acidic slurry was extracted with chloroform to determine whether any readily hydrolyzable fragments were present. Evaporation of the chloroform to approximately 1 ml and both gas chromatography and thin layer chromatography of the residue yielded no evidence of products.

TYPICAL INFRARED SPECTRUM OF MATERIAL FROM DEGRADED  
POLARIS BINDER CHROMATOGRAPHED ON  $\text{Al}_2\text{O}_3$  COLUMN



INFRARED SPECTRUM OF REACTION PRODUCT OF POLYPROPYLENE  
GLYCOL AND TOLUENE DIISOCYANATE

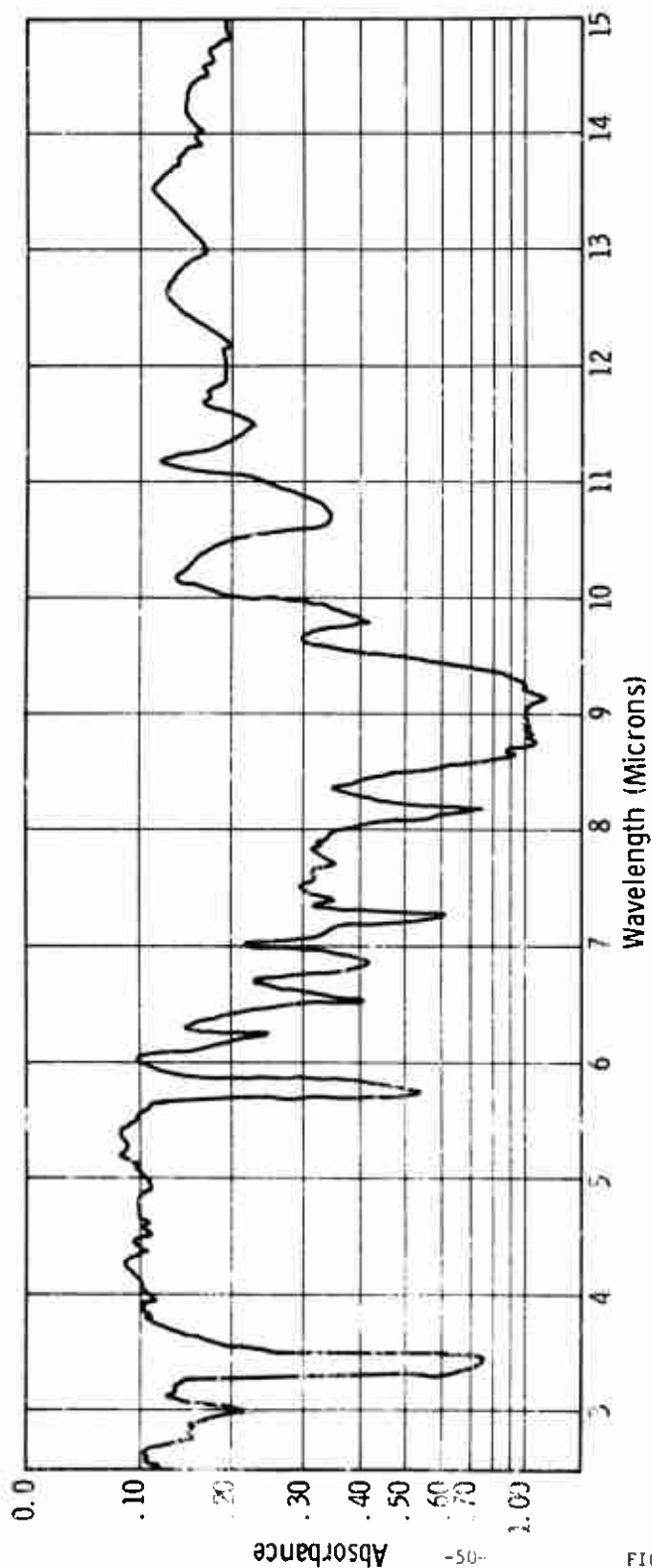
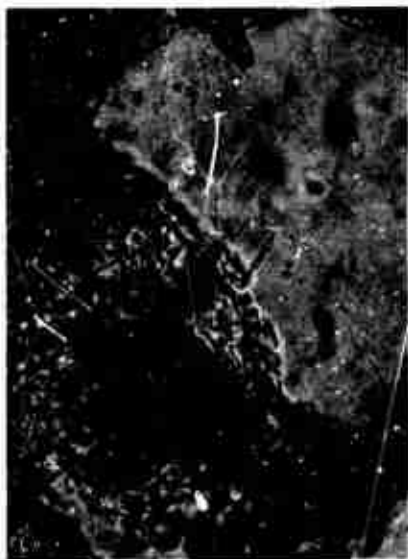


FIGURE 37

PHOTOMICROGRAPHS OF THE SEPARATION OF  $\text{NH}_4\text{ClO}_4$  AND  
ALUMINUM FROM REACTION SITE FROM POLARIS CYCLING UNIT



a



b



c

X250



d

X1000

Neutralization of the aqueous acidic layer and extraction with chloroform, followed by concentration of the extract and gas chromatographic analysis of the residue, gave no evidence of the presence of amines or other basic fragments.

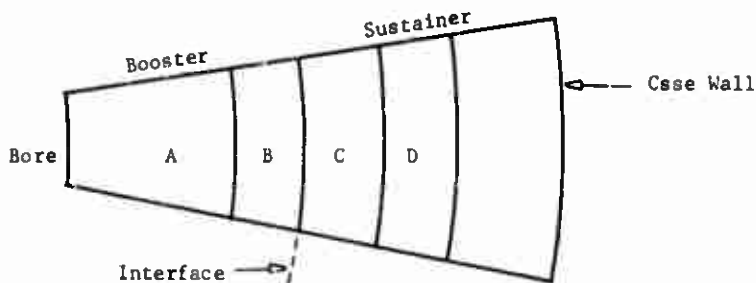
More severe hydrolytic conditions were next tried in order to cleave the high refractive index organic matter into smaller fragments. The organic matter was heated at 80°C for 4 hours with 25 ml of 2N NaOH after which most of the organic matter had gone into solution. The alkaline reaction solution was extracted five times with 50-ml portions of diethyl ether, and the ether was dried and concentrated to yield a very small amount of residue. An infrared spectrum of the residue revealed bands due to O-H and/or N-H and C-H bond absorptions, confirming the presence of hydroxy-terminated pre-polymer in the organic matter and that the high refractive index material was polyurethane polymer. The alkaline solution was made acidic and then extracted with chloroform; evaporation of the chloroform did not yield any residue.

#### C. CHEMICAL ANALYSIS OF HAWK PROPELLANT

The microscopic studies of aged samples of Hawk propellant had revealed that colored sites were formed in this bipropellant, and that the colors changed during the aging period. Migration of FeAA and/or plasticizer was the cause for these changes. The following experiments were done to confirm that this was indeed the cause for the color changes.

##### 1. Sample Preparation

A propellant sample from the 5-1/2 year old Hawk motor was analyzed for plasticizer and iron distribution. This propellant formulation contained 4.80% IDP and 0.06% FeAA in the booster and 4.20% trioctyl phosphate (TOP) and 0.10% FeAA in the sustainer.



One-inch thick sections from the booster-sustainer interface in each direction were cut out and designated Zone A, B, C, D, as illustrated above. A 100-g sample of each zone was cut into small pieces and soaked in



500 ml of methylene chloride for one week. The methylene chloride extracts, which contained FeAA and plasticizer, were decanted and analyzed.

To each of the residual swollen propellant samples was added a solution of 500 ml of water and 50 ml of 0.1N  $H_2SO_4$ . After three hours at 40°C, aliquots of the aqueous extracts were analyzed for any FeAA which had been converted to water soluble ferrous and ferric iron compounds during the 5-1/2 year storage period.

## 2. Methylene Chloride Extracts

### a. Analysis for Plasticizer

Analysis of the plasticizer content in Zones A to D was done by gas chromatography of equal aliquots of the methylene chloride extracts. A 2-ft column packed with 80 to 100-mesh glass beads coated with 5 wt% of silicone green rubber SE30 was used. A programmed heating rate of 15°C/min between 75-250°C gave the best separations. The results showed that Zone A contains predominantly IDP and Zone D predominantly TOP. On the other hand, Zone B showed a significant amount of TOP which had migrated from C, and Zone C contained proportionately an even larger amount of IDP that had migrated from B.

The plasticizer concentration gradients that originally existed in the booster and sustainer sections were the driving force for the migration across the interface. This migration of IDP into the sustainer and of TOP into the booster provided the liquid vehicles by which FeAA dissolved in the plasticizers was transported and redistributed. The resultant concentration and chemical identity of the redistributed FeAA was analyzed as follows.

### b. Analysis for FeAA

The spectrophotometric analysis of ferric iron can detect as low as 0.02 ppm (F.D. Snell and F. M. Biffen, "Commercial Methods of Analysis", Chemical Publishing Co., 1964, p 195). This method utilizes the reaction between ferric and thiocyanate ions to produce a complex ion with an absorption maximum at 475 mμ, which is a linear function of concentration.

The iron in the methylene chloride was FeAA, since ionic iron compounds would be insoluble. An aliquot from each of the  $CH_2Cl_2$  extracts was shaken with a measured amount of 0.5N  $H_2SO_4$  for 24 hours to convert the iron in FeAA to the ionic ferric state. An aliquot of the aqueous layer was reacted with KCNS and the absorbance measured in a Beckman DK2 spectrophotometer. Comparison with the absorbance of two ferric ion solutions of known concentration gave the amounts of FeAA in each zone. The results are given in Table IV. Virtually all the FeAA originally in the booster propellant had been converted into other forms while in the sustainer a small amount of FeAA migrated across the interface from C to B.

TABLE IV

## CHEMICAL ANALYSES OF HAWK SURVEILLANCE MOTOR

Original Composition, Wt. %		Booster		Sustainer	
	FeAA		0.06		0.10
	IDP		4.80		0.00
	TOP		0.000		4.20
Analyses		Zone A	Zone B	Zone C	Zone D
I.	Gas Chromatography	IDP trace TOP	IDP + TOP	TOP + IDP	TOP + trace IDP
II.	Iron Analyses, 10 <sup>3</sup> %				
	FeAA	>0.2	1.04	13.1	15.8
	FeAA converted to Ferric Salts	>1.3	>3.1	21.4	20.6
	FeAA converted to Ferrous Salts	8.2	16.9	6.6	2.5
	Iron unaccounted <sup>a</sup>	55.3	39.0	55.9	61.1
	Initial FeAA	60	60	100	100

<sup>a</sup>Not Extracted by CH<sub>2</sub>Cl<sub>2</sub> or aqueous H<sub>2</sub>SO<sub>4</sub>; may be iron oxides.

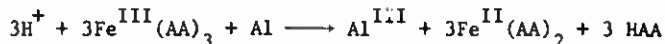
### 3. Aqueous Extracts

This extraction removed all the iron compounds soluble in the 0.1N  $H_2SO_4$ . Both ferrous and ferric iron would be extracted by this process. The thiocyanate method was first used to determine the amount of ferric iron in the extract. Then a few drops of hydrogen peroxide were added to convert ferrous iron to ferric and the mixture was reanalyzed. An increase in absorbance would be due to ferrous ion which had been oxidized by the peroxide to ferric ion. The results from these analyses are given in Table IV. The iron existed predominantly in the ferrous state in the booster, where aluminum, a good reducing agent, is also present, whereas the ferric state was more common in the sustainer, where there was no aluminum.

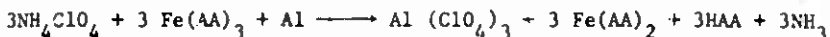
#### D. MECHANISMS OF IRON MIGRATION AND CHEMICAL CHANGES

The analysis of the Hawk propellant system established that plasticizers (IDP and TOP) migration across a bipropellant interface occurred to a significant degree and that these plasticizers were the liquid vehicles for the migration of iron acetylacetonate (FeAA) and other compounds. The ultimate fate of the FeAA was dependent upon whether aluminum was available for chemical reaction. Where available, Al reduced the iron in FeAA from the ferric to the ferrous state. In the absence of Al, the FeAA remained more stable, but after ambient storage of the propellant for up to 5-1/2 years much of the iron was converted to unextractable forms such as the oxides or the metal. The mobility of FeAA and the oxidation-reduction between Al and FeAA might lead to side effects, such as influencing the chemical stability of the binder or of compounds derived from the binder which are susceptible to oxidation-reduction. Further oxidation-reduction of the binder would lead to lower propellant stability.

The reactions leading to the conversion of FeAA to other forms are presented below. While these reactions are postulated in a sense that direct evidence for them is not available, all the reactions are ones which are known to occur in propellants, are favored thermodynamically, and are consistent with the chemistry of the system. The iron is reduced by the aluminum, thus



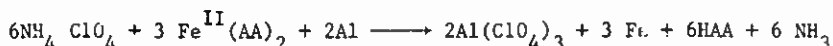
The acid is provided by the ammonium perchlorate and the aluminum is converted to aluminum perchlorate. The complete reaction is



The acetylacetonate (HAA) undergoes further reaction with the ammonia to give imine and heterocyclic compounds. This reaction is slow in a propellant

medium which is non-aqueous and requires prior etching of the aluminum oxide coating of the metal. Scratching of the oxide coating of the aluminum during propellant mixing is well known.

The reduction may go even further and give iron metal.



Whether this last reaction actually occurs is not known. Tests for metallic iron were not made, but this reaction along with the formation of iron oxide would explain presence of unextractable iron compounds.

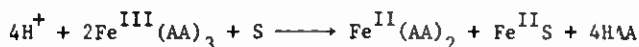
The reduced iron found in the sustainer where no aluminum is present indicates the presence of other methods of reduction. Two possibilities exist. The first involves reduction by the antioxidant



The antioxidant in the sustainer is an uncharacterized phenylene diamine derivative, BLE, but it can take up the electron and cause reduction of the iron. The proton is provided by the  $\text{NH}_4\text{ClO}_4$ . The second possibility is reduction by propionaldehyde, a degradation product of the polypropylene glycol (Gaylord, "Polyethers", Interscience Publishers, 1963, p 147).



Reduction in the booster may also occur by sulfur which is present.



The sulfur tends to precipitate the iron as a sulfide which is rather inert. The scavenging of metals to an innocuous sulfide is believed to be the beneficial effect of sulfur in these propellants.

While the iron is reduced, much of it is converted to ionic compounds by the breakdown of the acetylacetonate. One of the most direct reactions for this is reaction with aluminum alkoxides



The  $\text{Al}(\text{AA})_3$  is more stable and less soluble than  $\text{Fe}(\text{AA})_3$  and provides a driving force for the reaction. The presence of  $\text{Al}(\text{OR})_3$  type compounds in the propellant has been substantiated by other workers (see next section).  $\text{Fe}(\text{AA})_2$  behaves similarly.

In general the iron chelates can be converted to the insoluble hydroxides in the presence of moisture and an acceptor for acetylacetone. Unless the acetylacetone is removed, the equilibrium favors the formation of the chelate. Thus



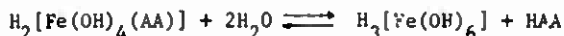
The HAA is removed by reaction with  $\text{NH}_3$  formed from the amine crosslinker, triethanolamine, and  $\text{NH}_4\text{ClO}_4$



and by reaction with  $\text{CuO}$  in the burning additive.

Compounds of the type  $\text{H}[\text{Fe}(\text{OH})_2(\text{AA})_2]$  are well known acids (Meerwein, Ann. Chem. 45, 227 (1927); 476, 113 (1929); 484, 113 (1930)). Oberth (J. Org. Chem., 31, 887 (1966)) has postulated that a similar compound  $\text{H}[\text{Fe}(\text{OR})_2(\text{AA})_2]$  to be the active catalytic species in the FeAA catalyzed isocyanate alcohol reaction.

By successive addition of water and displacement acetylacetone the iron is converted to  $\text{Fe}(\text{OH})_3$  and  $\text{Fe}(\text{OH})_2$ .



Similar reactions may be written for  $\text{Fe}(\text{AA})_2$ .

## 1. Stability of a Model Urethane and a Model Urea

The stability of a model urethane and a model urea in contact with  $\text{NH}_4\text{ClO}_4$ ;  $\text{NH}_4\text{ClO}_4$  and Al;  $\text{NH}_4\text{ClO}_4$ , Al and FeAA; and  $\text{NH}_4\text{ClO}_4$ , Al, FeAA, and copper chromite was studied. Two solutions of dimethoxyethane (glyme) containing ethyl carbanilate (10 wt%) and dimethylurea (10 wt%) were prepared and 0.5-g aliquots were separately mixed with about equal weights of the four solid propellant combinations. The mixtures were sealed in glass vials and stored at 50°C. At intervals, the concentration of ethyl carbanilate and of dimethylurea was determined by gas chromatography. A 2-ft column packed with 60-80 mesh Diatoport-S coated with 10 wt% of silicone green rubber SE30 was used and a programmed heating rate of 15°C/min between 75-200°C allowed separation of the model compound from the phenylcyclohexane internal standard. Analyses showed that even after 14 days at 50°C, both the urethane and the urea remained intact in all environments. This showed that direct chemical reaction between FeAA and Al did not lead to chemical reactions of the functional groups of a polyurethane binder and that other factors were responsible for the reactions leading to the aging sites.

The absence of chemical changes in this study of the model compounds was unexpected, in view of the observation that microscopic examination of model propellant grains had shown that aging site formation occurred after about 2 weeks storage. An explanation for this discrepancy is the differences in surface condition of the aluminum present in the two cases. The aluminum is normally coated with oxide and in this form is relatively unreactive. From studies made at Aerojet several years ago, Dr. A. E. Oberth concluded that during propellant mixing the aluminum oxide coating was scratched clean. He postulated the reaction of this clean active surface with glycols formed aluminum alkoxides and indicated that this was the cause of "soft-center" cures. In a further study Dr. R. Olberg showed that the soluble aluminum (alkoxide form) increased with length of mixing, solids content, and type of glycol. While neither of these workers dealt with the effect of these aluminum alkoxides on the stability of the binder, the probability of such interaction is certainly good. The chemical study of the urethane and urea stability in the presence of propellant solid ingredients indicated only the effects of the oxide-coated aluminum because aluminum free of the oxide coat is very difficult to obtain and maintain. The reaction involved was



## E. CHEMICAL ANALYSIS OF A PBAN-EPOXIDE PROPELLANT

Procedures and techniques developed for the chemical analysis of degraded binder from an aged Polaris polyurethane propellant were used to analyze a PBAN-epoxide Minuteman propellant, Thiokol TPN 1011. A propellant section which had been stored for 4 years at ambient conditions was used for this work. The binder system of this propellant was composed of a butadiene-acrylonitrile-acrylic acid terpolymer (PBAN) cured with an epoxide, ERL 2274,

and contained no other organic component. Microscopic examination of thin sections of this propellant did not reveal any reaction sites similar to those found in the Polaris polyurethane propellant. In fact, other signs of chemical change were not optically apparent.

A 100-g sample of the PBAN propellant was cut into small pieces and extracted with 500 ml of ethylene dichloride for 48 hours at 25°C. The solvent was decanted and concentrated to give 5 wt% of residue, which is about 35 wt% of the total binder. Gas chromatographic analysis of a  $\text{CHCl}_3$  solution of residue through a 2 ft x 1/4 in. I.D. column of glass beads coated with 5 wt% of silicone gum rubber SE30 revealed at least 10 major components when temperature programmed from 100-300°C. The residue was successively triturated with hexane, cyclohexane and benzene to achieve a preliminary separation into Fractions A, B, and C, respectively. These materials looked similar to the initial residue. Thin layer chromatography of each fraction revealed that Fraction A was resolved into 3 fractions, while Fractions B and C were each separable into 2 components. These separations were more effective using silica gel paper than with paper coated with alumina, demonstrating that acidic fragments were present. These results led to attempts to isolate by gas chromatography and to identify by infrared spectroscopy some compounds of the mixture. Fraction B was subjected to gas chromatography through a 2 ft x 1/4 in. I.D. column of glass beads coated with SE30 and temperature programmed between 100-300°C at the rate of 11°C/min. Under these conditions, the column resolution was not sufficient to allow clean separation of components. Instead it was arbitrarily decided to collect 3 fractions over the column temperature ranges of 100-200°, 200-250°, and 250-300°C, respectively. Compounds which emerged from the column at each of these temperature zones were collected on precooled infrared cell plates and spectra were recorded. The spectra of all three of the fractions were essentially identical; the main features were the presence of a band at 4.50 $\mu$  due to cyano group absorption and at 5.85 $\mu$  due to carbonyl absorption.

This data showed that low molecular weight fragments containing cyano and carboxyl groups were present in the propellant, suggesting that increased hardening that occurs with PBAN propellants upon aging was caused in part by slow volatilization of low molecular weight fragments which had functioned as plasticizer. To test this possibility, samples of some PBAN propellant were placed in a 130°F oven for 3 weeks and for 8 weeks and the chemical analyses were repeated. The amount of sol fraction increased to 50 wt% (3-week sample) and to 61 wt% (8-week sample), whereas the original sample stored at ambient conditions was reanalyzed and contained 35 wt% sol fraction, same as the original value.

A gas chromatography analysis of the sol fraction from the 8-week 130°F sample followed by infrared sampling of the effluent stream showed that the chemical composition was similar to the earlier results, except that a higher proportion of lower molecular weight fragments were now obtained, indicating that no detectable chemical transformations leading to coupled and

higher molecular weight fractions had occurred. Apparently, bond scission was the sole result of longer term heating. Within the time span of the test period, degradation of the binder increased and produced a higher proportion of lower molecular weight fragments. However, these degradation products were still not volatile enough to escape from the binder and this volatile component mechanism could not account for the aging hardness.



### III. MECHANICAL AND BALLISTIC PROPERTIES AND REACTION SITES OF PROPELLANTS

#### A. THE HAWK PROPELLANT SYSTEM

Model grains of the Hawk bipropellant system were prepared and the formation of color sites was monitored. The sites were found to be generated randomly and upon further storage were redistributed with a majority of the sites localized in the booster section near the bipropellant interface. The pathway of this redistribution was established by chemical analysis to be plasticizer and FeAA migration. Migration of the latter and chemical conversions of it into non-chelated ferrous and ferric iron led to the different colors of the reaction sites. The effects of these reactions upon the propellant properties of Hawk field motors are shown in Tables V to VII. Examination of the data shows that the increase in reaction sites on aging did not affect propellant properties. The changes in tensile strength of either the booster or sustainer showed no significant trend towards deterioration upon aging up to 6.5 years.

Changes in mechanical properties caused by reaction site formation would have been expected to be revealed, if at all, by a change in bipropellant bond strength, since this area was subjected to the greatest influence of plasticizer and FeAA migration. Table VII shows that even in this propellant zone, no deterioration of mechanical properties had occurred. Thus reaction site formation was not correlatable with aging over the length of time considered here. However, the reaction sites may still be a portent of future failure of the propellant.

#### B. THE POLARIS AND MINUTEMAN IGNITER PROPELLANT SYSTEMS

Initial interest in the Polaris propellant developed from the visible degradation of a field aged motor which had a 1/2 in. layer of degraded propellant near the bore surface. Table VIII shows the significant extent to which this degradation had lowered the mechanical properties at the surface and altered the burning rate. Microscopic examination of thin sections of this degraded zone revealed the presence of reaction sites. The question arose whether the reaction sites could be correlated with propellant degradation and thus be a method for monitoring storage life.

The data from the mapping of reaction sites in the model Minuteman Igniter grains showed that site formation was inversely temperature dependent between 110-180°F. We interpret this to mean that the formation of reaction sites was caused by intermediates which were unstable at higher temperature and were destroyed before having time to form reaction sites. The chemical identity of one of these reaction intermediates was postulated to be aluminum alkoxide formed by the reaction of the polyol portion of the polyurethane prepolymer with freshly created Al surfaces exposed by the abrasive action during propellant mixing. Indirect evidence in support of the importance of

TABLE V

## MECHANICAL PROPERTIES OF FULL SCALE HAWK FIELD MOTORS

Booster Propellant ANP 2830 Mod I

	$\sigma_m$ , psi	$\epsilon_m$ , %	$\epsilon_b$ , %	$E_o$ , psi
Initial	128	47	53	462
Aged 3.5 yrs	167	39	47	636
% Change	+30	-17	-11	+37
Initial	145	57	62	343
Aged 4.5 yrs	176	29	34	873
% Change	+21	-49	-45	+154
Initial	143	31	36	656
Aged 5.5 yrs	155	28	35	824
% Change	+8	-10	-3	+25
Initial	146	52	56	484
Aged 6.5 yrs	156	33	40	801
% Change	+7	-37	-28	+66

TABLE VI

## MECHANICAL PROPERTIES OF FULL SCALE HAWK FIELD MOTORS

Sustainer Propellant ANP 2832 Mod I

	$\sigma_m$ , psi	$\epsilon_m$ , %	$\epsilon_b$ , %	$E_o$ , psi
Initial	64	6	28	1429
Aged 3.5 yrs	105	6	15	2404
% Change	+64	0	-46	+67
Initial	71	7	25	1300
Aged 4.5 yrs	88	8	18	1506
% Change	+24	+14	-28	+16
Initial	71	6	22	1710
Aged 5.5 yrs	58	6	31	1446
% Change	-18	0	+41	-15
Initial	64	6	28	1429
Aged 6.5 yrs	99	6	14	2539
% Change	+55	0	-50	+78

TABLE VII

## MECHANICAL PROPERTIES OF FULL SCALE HAWK FIELD MOTORS

## Bipropellant Tensile Bond at the Interface

	$\sigma_m$ , psi	$\epsilon_m$ , %	$\epsilon_b$ , %	$E_o$ , psi
Initial	60	17	14	930
Aged 3.5 yrs	72	11	14	935
Aged 4.5 yrs	64	11	12	958
Aged 5.5 yrs	65	8	10	1012

TABLE VIII

MECHANICAL PROPERTIES OF POLARIS PROPELLANT ANP-2639  
AGED 65 MONTHS IN FIELD

	Unaged	Surface	Position of Aged Sample				
			From Core			From Wall	
			1/2"-1-1/2"	1-1/2"-3"	3"-8"	8"-4"	4"
$\sigma_m$ , psi	90	35	78	87	91	83	90
$\epsilon_m$ , %	100	148	118	113	98	98	94
$\epsilon_b$ , %	155	192	164	161	149	158	151
$E_o$ , psi	264	103	183	226	262	250	267
Burning rate in./1000 psi	0.234	0.288	--	--	0.280	--	--

activated Al surfaces was given by the inability to induce formation of reaction sites when hand mixing of an identical propellant formulation yielded no reaction sites after an identical storage period. The identification of reaction sites to be polyurethane polymer was established by chemical analysis of a batch of isolated reaction site particles. The fact that the sites were optically different from the remaining binder cannot be explained.

As seen from Table IX, no significant change in mechanical properties had occurred after 18 months at 110°F, even though reaction site formation was detected after only 3 months and had increased to about 1 vol % after 6 months. This supports the previous conclusion that if reaction site formation is related to aging, the sites precede actual evidence of mechanical aging by a considerable time interval.

TABLE IX

MECHANICAL PROPERTIES OF MODEL  
MINUTEMAN IGNITER PROPELLANT ANP-2758 Mod II

	<u>Initial</u>	<u>Aged 6 Months at 110°F</u>	<u>Aged 18 Months at 110°F</u>
$\sigma_m$ , psi	105	97	102
$\epsilon_m$ , %	63	66	60
$\epsilon_b$ , %	78	85	82
$E_o$ , psi	442	467	478

#### IV. SUMMARY

##### A. THE MECHANISM OF SITE FORMATION

The intimate relation between the FeAA, aluminum, and ammonium perchlorate leads to the conclusion that these three are initially the nucleus from which the site develops. The FeAA becomes adsorbed on the aluminum surface by polar attraction and when the combination comes in contact with  $\text{NH}_4\text{ClO}_4$  which is present in high concentration, the site formation begins. The first reactions involve the reduction of the FeAA on portions of the aluminum surface which have been etched free of the oxide coat either by chemical action or by the mechanical scratching during mixing. This reaction is immeasurably enhanced by the presence of water which dissolves the FeAA and the acidic  $\text{NH}_4\text{ClO}_4$  on the surface of the aluminum. The water is initially introduced with the ammonium perchlorate (up to 0.05% of the oxidizer) and later by diffusion from the external environment. With time the iron is reduced and/or converted to other iron compounds. The site becomes more polar in character because it becomes a site for accumulation of moisture,  $\text{NH}_3$ , and acetyletone which form along with the site. The combination of polar compounds tend to dissolve ammonium perchlorate. At this stage a slow hydrolytic attack begins to occur on the polyurethane binder surrounding the site. The polymer by hydrolysis is changed from a soft elastomer into a gelatinous mass which expands constantly into the untouched regions of the binder.

This mechanism explains why the components of the propellant can form the sites in a random fashion without help from the environment. However, since moisture greatly increases the rates of the reactions involved, diffusion of moisture from the environment can cause a concentration of sites on the surface. Similarly, concentration of sites at the booster-sustainer interface of Hawk propellant was caused by a replenished supply of FeAA by migration with the plasticizer across the interface. The distribution of sites is, thus, explained by a consideration of the migration patterns of the ingredients on a day to day, year to year basis.

While the aluminum surface is scratched clean by the mechanical action of mixing, the slow etching of the aluminum surface over a long period of time is the principal method of initiation for reaction sites. The mechanically cleaned aluminum surface is important during accelerated aging. Since the clean surface can react with moisture, alcohols, and air, higher temperature favors the reaction of these agents with the aluminum. For this reason the accelerated aging at higher temperature showed a decrease in reaction site formation.

The reactions of the FeAA are not directly connected with the degrading of binder. Rather the reactions serve to produce polar molecules which dissolve the ammonium perchlorate and water and create a hydrolytic medium. This is not to exonerate FeAA completely for it is known that FeAA will catalyze the high temperature degradation of polyurethanes.

While all the chemical reactions have not been proved by the data gathered, all the reactions (shown in the preceding sections) are known, well-documented, and entirely consistent with the chemistry of the systems. Many questions remain unanswered because enough aged propellants of many different varieties were not available for study. It is shown that aging was occurring in PBAN-epoxide propellant, but no aging site as such could be optically observed. No data are presently available for hydroxy-terminated PBD propellants.

#### B. RECOMMENDATIONS

More stable propellants could be obtained by use of a more stable catalyst or by a binder which dissolves less water (as, for instance, the PBD type), but it is likely that this measure will only forestall aging temporarily. The real culprit is moisture which behaves as a reactant and as a catalyst for aging reactions. In this respect, the conclusion is not new, but is vividly brought to the fore. Motors made in dry conditions (no matter what the cure system since all are vulnerable) and sealed against the ingress of moisture offer the best method of increasing the life of present propellants.

It is recommended that monitoring of reaction sites be continued as an indication of aging. While the lack of very old propellant grains and the high stability of the propellant studied prevented the correlation of reaction site concentration and the loss of mechanical and ballistic capability, it is logical that the aging of the propellant around the aging site would eventually affect the propellant capability. The sites are a very early indicator of propellant aging.

#### C. EXPERIMENTAL TECHNIQUES

In the course of this study microscopic and chemical analytical techniques were adapted for the particular study of propellants. Microscopic examinations were very useful in instances where optical characterizations were required, especially when polarized lighting and dark phase contrast techniques permitted studies which could not be done under ordinary light. The mapping of reaction sites and subsequent derivation of contour lines yielded valuable information on areas of highest reactivity which in turn provided clues on the identity of some of the reactive species.

For the chemical analysis performed in this study, both wet analyses and instrumental methods were successfully used. Thin layer chromatography was useful for rapid monitoring of different fractions that were obtained from the complex degraded binder samples. An especially attractive feature of TLC technique was that extremely small sample sizes were required. The combination of microscopic observation, isolation by use of the micro-manipulator attachment, and analysis by TLC was a very effective one for the type of study required during this program. For more precise and quantitative work, gas chromatographic analysis was used, as in the case of determining

plasticizer migration in the Hawk bipropellant system. Confirmation of the identity of compounds that were separated by gas chromatography was made by infrared spectroscopy and comparison of the spectra with the spectra of known compounds.

Another valuable spin-off of this work is the development of techniques for chemical analysis of very small portions of propellant. These techniques apply to analyses of mixing and curing reactions as well as to aging. Because of this their application would be very useful to solving of specific problems which arise often in the course of propellant processing.



UNCLASSIFIED

Security Classification

## DOCUMENT CONTROL DATA - R &amp; D

(Security classification of title, body of abstract and indexing annotation must be entered when the overall report is classified)

1. ORIGINATING ACTIVITY (Corporate author) Aerojet-General Corporation P. O. Box 15847 Sacramento, California		2a. REPORT SECURITY CLASSIFICATION None
		2b. GROUP
3. REPORT TITLE  MICROSCOPIC AND MICROCHEMICAL STUDY OF AGED SOLID PROPELLANT GRAINS		
4. DESCRIPTIVE NOTES (Type of report and inclusive dates) Final Report		
5. AUTHOR(S) (First name, middle initial, last name) Di Milo, Anthony J Moe, Henry McGurk, James L.		
6. REPORT DATE	7a. TOTAL NO. OF PAGES 78	7b. NO. OF REFS None
8a. CONTRACT OR GRANT NO. AF 04(611)-11637	8b. ORIGINATOR'S REPORT NUMBER(S)  1083-81-F	
b. PROJECT NO. 3148		
c.	9b. OTHER REPORT NO(S) (Any other numbers that may be assigned this report)	
d.		
10. DISTRIBUTION STATEMENT This document is subject to special export controls and each transmittal to foreign governments or foreign nationals may be made only with prior approval of AFRL (RPPR-STINFO), Edwards, California 93523		
11. SUPPLEMENTARY NOTES	12. SPONSORING MILITARY ACTIVITY Air Force Rocket Propulsion Laboratory Research and Technology Operations Edwards, California	
13. ABSTRACT  Air Force Systems Command United States Air Force  Microscopic examination of thin sections of aged polyurethane propellant from a field aged Polaris motor revealed the presence of high refractive index reaction sites surrounding aluminum particles. Chemical analyses of these sites revealed them to be composed of polyurethane binder. Color sites in a Hawk field aged motor were found by microscopic examination and chemical analysis of these sites showed them to be due to the presence of iron in different oxidation states. The source of the iron is the iron acetylacetonate used as a curing catalyst.  Model propellant grains were made to simulate conditions for the generation of reaction sites and the formation and growth of the sites were followed by mapping. Correlation of reaction site formation with mechanical properties of the propellant was unsuccessful because the propellants available for study (up to 7 years old) showed no real loss of mechanical and ballistic capability. The reaction sites portend changes which will occur over a period of time not now available for study.  The chemical mechanism of the aging was defined and expressed by chemical equations.		

UNCLASSIFIED

Security Classification

14.	KEY WORDS	LINK A		LINK B		LINK C	
		ROLE	WT	ROLE	WT	ROLE	WT
	Grain Aging Propellant Aging Microscopic Techniques Hawk Aging Polyurethane Aging Polaria Aging Minuteman Igniter Propellant Aging Aging Reaction Sitea Mechaniam of Aging of Polyurethane Propellants Aluminum Reactions of Aging of Propellanta FeAA in Hawk Propellant Chemical Reactions in Aging Analytical Methods in Aging Study						

UNCLASSIFIED

Security Classification